NASA TECHNICAL NOTE

NASA TN D-5339

c. 1

NASA TN D-5339

ANALYSIS OF THE DYNAMIC RESPONSE OF LIQUID JET ATOMIZATION TO ACOUSTIC OSCILLATIONS

by Marcus F. Heidmann and John F. Groeneweg

Lewis Research Center
Cleveland, Ohio

NATIONAL AERONAUTICS AND SPACE ADMINISTRATION • WASHINGTON, D. C. • JULY 1969

ANALYSIS OF THE DYNAMIC RESPONSE OF LIQUID JET ATOMIZATION TO ACOUSTIC OSCILLATIONS

By Marcus F. Heidmann and John F. Groeneweg

Lewis Research Center
Cleveland, Ohio

NATIONAL AERONAUTICS AND SPACE ADMINISTRATION

For sale by the Clearinghouse for Federal Scientific and Technical Information
Springfield, Virginia 22151 – CFSTI price $3.00

ABSTRACT

An atomization model prescribing jet breakup when jet distortion caused by aerodynamic forces attains a critical value is used to analytically and numerically evaluate the atomization rate perturbations caused by acoustic oscillations. The varied dynamic response within traveling, standing, and radial transverse acoustic modes is presented. An amplifying effect of a steady tangential velocity on dynamic response is also examined and compared with experimental evidence. The results generally imply that jet atomization dynamics can significantly affect the stability of a rocket engine combustor.

ANALYSIS OF THE DYNAMIC RESPONSE OF LIQUID JET ATOMIZATION TO ACOUSTIC OSCILLATIONS

by Marcus F. Heidmann and John F. Groeneweg

Lewis Research Center

SUMMARY

The dynamic behavior of an axial liquid jet within traveling, standing, and radial transverse acoustic modes in cylindrical chambers is examined analytically and numerically for dynamic properties useful in characterizing a combustion process for stability analysis. An atomization process is used which prescribes jet breakup when jet distortion caused by aerodynamic forces attains a critical value. Two response factors are evaluated: the in-phase N_R and out-of-phase N_I components of the atomization rate perturbations with respect to pressure perturbations. Effects of acoustic oscillations on jet breakup time are also determined. In general, the results imply that jet atomization dynamics can significantly affect the stability of a rocket-engine combustor.

The response factors N_R and N_I are converging periodic functions of a characteristic breakup time $\omega\bar{\tau}$ with peak value dependent on acoustic conditions. Considering pressure oscillations alone, peak values approach unity. Including a velocity perturbation in-phase with the pressure elevates the peak values by a factor of 3/2; an out-of-phase velocity perturbation reduces the peak by 1/2. Velocity oscillations also reduce the mean jet breakup time and, thereby, affect the characteristic time $\omega\bar{\tau}$ of the process.

Spatial variations of acoustic properties within a given mode can cause large variations in local dynamic properties of the atomization process. The effect on the response factors of the varied velocity and pressure patterns within a specific mode precludes any simple characterization of dynamic properties. However, the response factors for the traveling mode can be larger than those for either the standing or radial modes.

The amplifying effect of a steady vortex velocity on the response in a traveling mode is substantial. Peak values of the response factor can increase by an order of magnitude. The results appear to be consistent with experimental studies of combustion instability with such vortex flow.

INTRODUCTION

In the theoretical analysis of acoustic mode instability in rocket-engine combustors, the dynamic properties of the combustion process represent important initial assumptions which substantially affect the solutions for system stability. Also, in the phenomenological approach to instability, the combustion process represents the energy source which sustains the acoustic oscillations and becomes a prime target in any attempt to stabilize the system. Characterization of the dynamic behavior of the combustion process, therefore, is not only useful but at times must precede an attack on the problems of instability.

Complete characterization of the many facets of the actual combustion process in a rocket engine and the integration of them into a comprehensive model of the overall system appears improbable. Instead, dynamic behavior of one or a combination of several processes comprising the overall combustion process is frequently employed to simulate combustion dynamics. Atomization, vaporation, mixing, chemical kinetics, drop shattering, and recirculation are among the individual processes which require attention in liquid-propellant engines. Theoretical analyses of the dynamic behavior of individual processes are particularly helpful in deciding which process or combination of processes can best characterize combustion. The analysis of droplet vaporization (refs. 1 and 2), for example, has shown a significant response of the vaporization rate to acoustic oscillations. This response, coupled with the concept of a vaporization limited combustion process, can be used to characterize the combustion process in certain engines.

Similarly, the analysis of the response of a gaseous hydrogen injection system to acoustic oscillations combined with the oxygen vaporization response (refs. 5 and 6) also provide physical insight into the dynamic properties of the combustion process. In this report an attempt is made to expand this insight of combustion dynamics by analyzing the dynamic behavior of the breakup or atomization of liquid jets.

Perturbations in atomization rate caused by acoustic oscillations are of particular importance when, as observed in some experimental tests (refs. 7 and 8), extremely small drops are formed which burn rapidly. The atomization process may then be the rate controlling process in the dynamic system. The low surface tension of such liquids as oxygen or severe pressure oscillations (produced naturally or by explosives used in dynamic testing) are two conditions conducive to the formation of small drops and combustion instability dependent on atomization dynamics.

The liquid jet breakup or atomization model developed by Clark (ref. 9) is used for the analysis of jet dynamics. Although elementary in concept, the model expresses the instantaneous jet properties during breakup - a necessary prerequisite for an unsteady

analysis of any process. The analysis emphasizes transverse acoustic modes in cylindrical chambers because of the prevalence of such modes in unstable rocket combustors. Approximate analytical solutions of the response of atomization rate to pressure oscillations are derived. These results are supported by numerical solutions which eliminate the simplifying assumptions used in the analytical procedures. The effects of a spatially distributed breakup process and vortex flow on dynamic behavior are also examined.

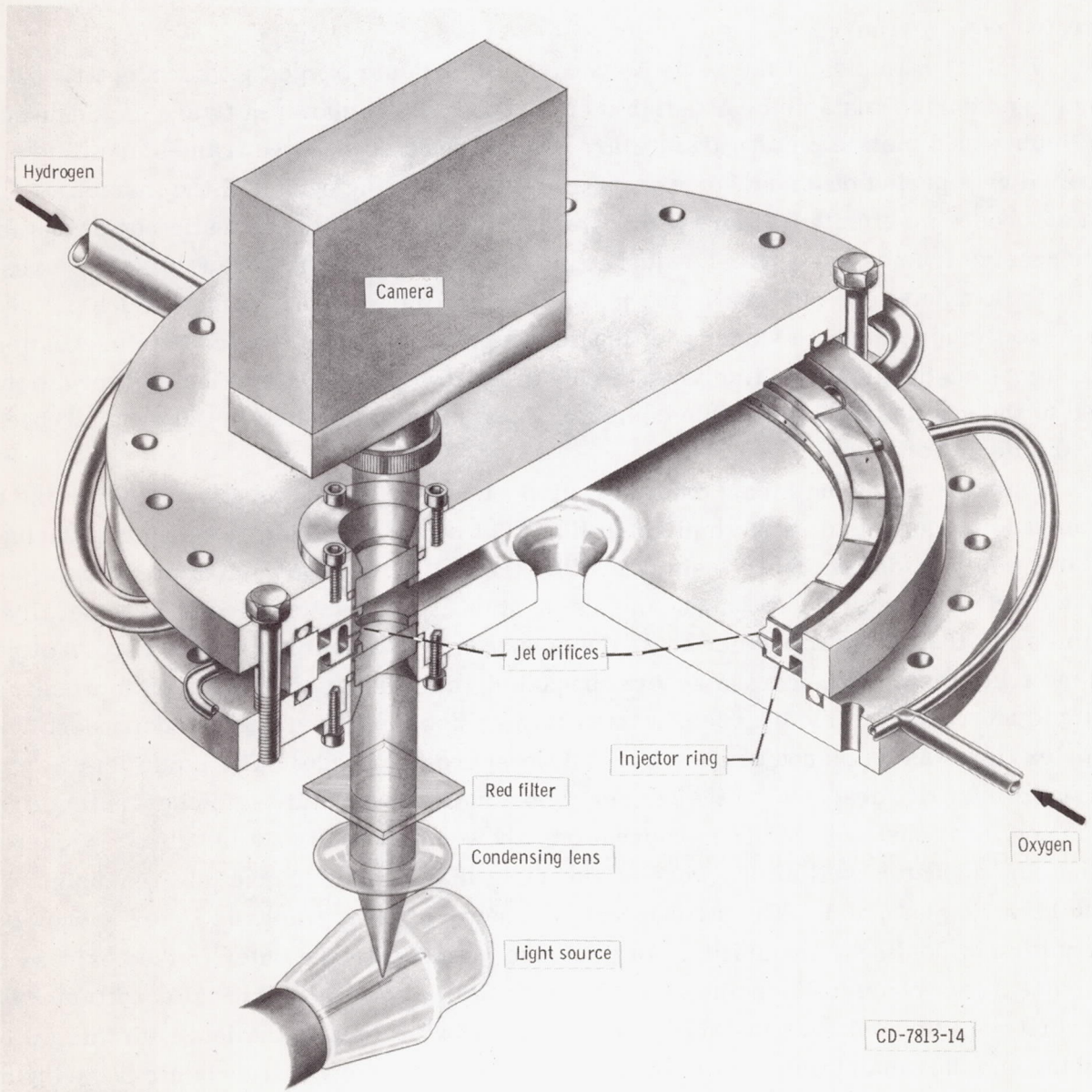

Figure 1. - Two-dimensional circular combustor and photographic arrangement.

OBSERVATIONS OF JET DYNAMICS

A review of some experimental observations of a liquid jet in a two-dimensional circular combustor will illustrate the type of dynamic behavior of interest in this analysis. Figure 1 typifies the experimental arrangement (ref. 8). Injected propellants and combustion gases flow radially inward from the circumference, and photographic observations are centered on a single injector element. Vortex flow within the cavity, induced by the tangential injection of a secondary gas, caused unstable combustion coupled to the first traveling transverse acoustic mode.

Typical examples of the periodic behavior of a liquid oxygen jet burning with gaseous hydrogen during unstable combustion (refs. 7 and 8) are shown in figure 2. Sequences of high-speed motion picture frames are shown where successive frames are time separated by a period differing somewhat from the oscillating period of the instability (a stroboscopic effect). Figure 3 illustrates the corresponding acoustic conditions for successive frames in a typical sequence. This stroboscopic technique resolves gross, rather than detailed, changes in the jet shape with time. Examination of such pictures, however, showed a time varying jet length which is coupled to the acoustic oscillations. Such jet-length variations imply variations in mass release rate. These observations led to the suspicion that unstable combustion was directly related to the dynamic behavior of the liquid jet.

Experiments using mixed oxides of nitrogen and hydrazine as propellants in the two-dimensional combustor also implicated liquid jet behavior as vitally important during unstable combustion. In these tests (ref. 10), the impingement of unlike propellant jets was used for injection. Although combustor stability characteristics were generally similar to the hydrogen-oxygen test, the occurrence of a nonlinear instability is of particular interest. Although the general behavior was a linear instability with pressure amplitude related to the degree of vortex flow, a nonlinear instability independent of the vortex flow was triggered above a critical pressure amplitude. The liquid jets were photographically observed in the neighborhood of this threshold region separating linear and nonlinear instability. The observations showed that nonlinear instability occurred when the acoustic oscillations were of sufficient magnitude to cause jet breakup prior to the impingement point. The stroboscopic sequence of photographs in figure 4 show a condition of nonlinear instability. In this case, breakup of the outer (mixed oxides of nitrogen) jets prior to the point of impingement appears to be a critical condition. The severity of this nonlinear instability was reduced by protecting the jets with thin walled tubing and thus maintaining impingement. These tests imply that dynamic behavior of the jet breakup process determines not only the threshold condition for nonlinear instability but that the acoustic gains associated with simple jet atomization are larger than those associated with impinging jet atomization.

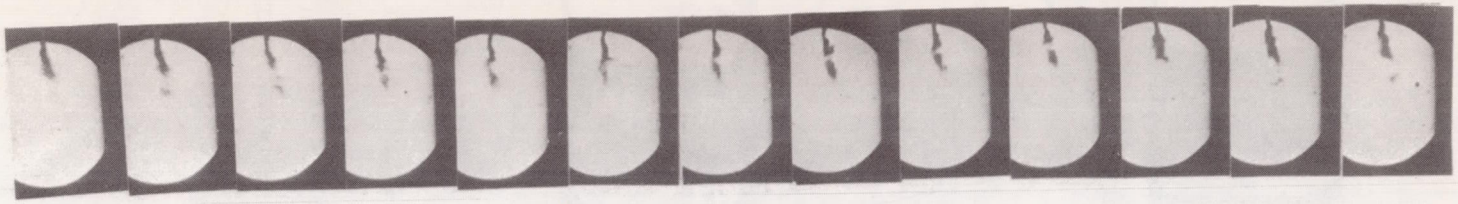

(a) Pressure amplitude, 20 percent; low oxygen jet velocity.

(b) Pressure amplitude, 10 to 20 percent.

(c) Pressure amplitude, 5 to 10 percent.

(d) Pressure amplitude, 5 percent; high oxygen jet velocity.

Figure 2. - Liquid oxygen jet behavior with first transverse mode of instability (ref. 7).

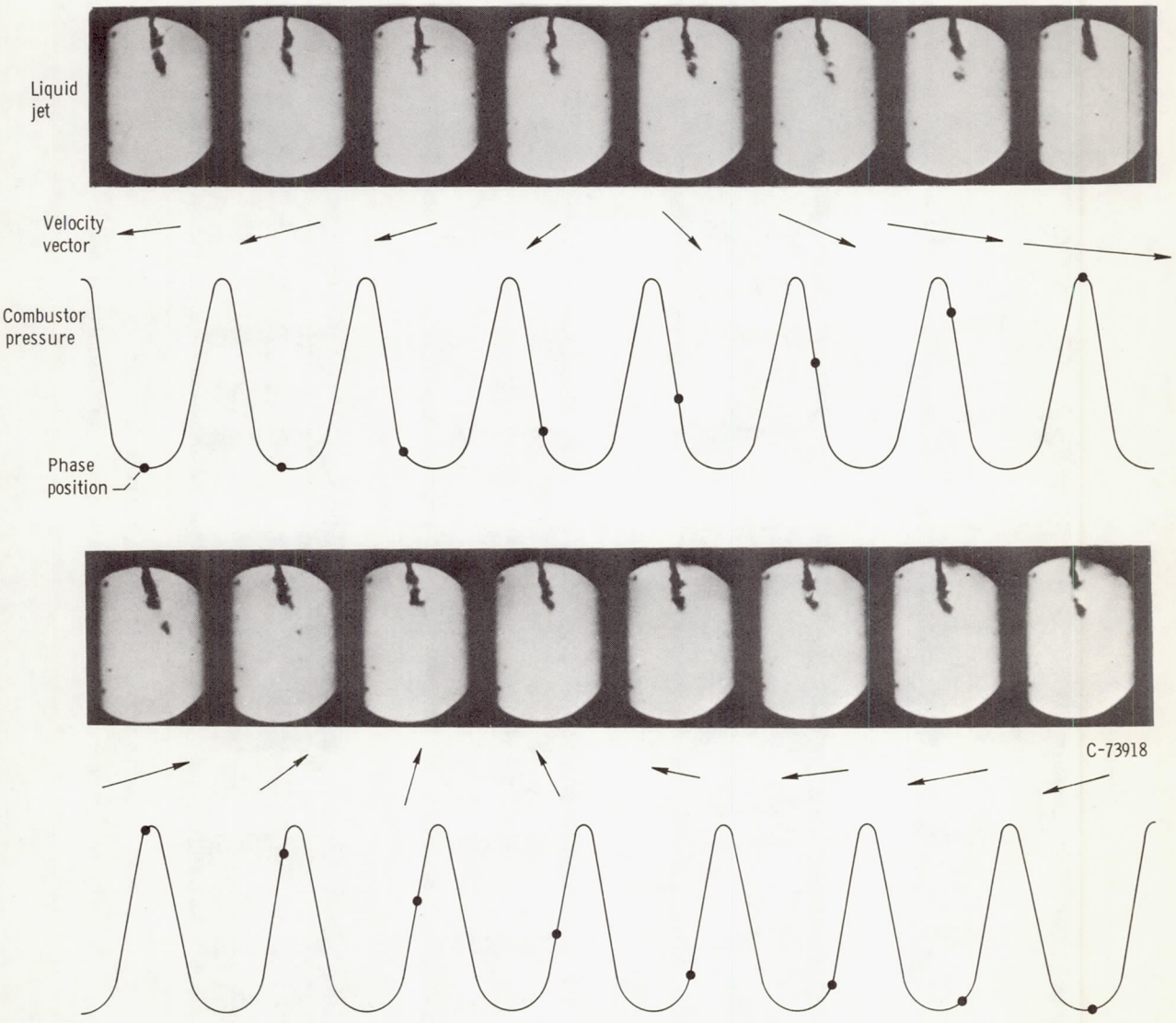

Figure 3. - Velocity vector and phase position for sequence of jet photographs (ref. 8).

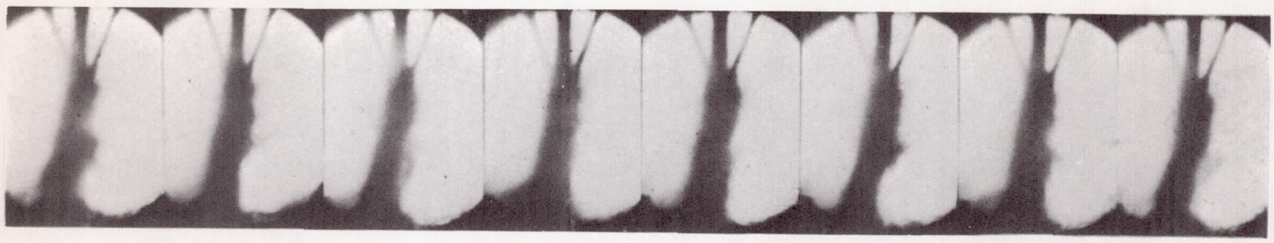

(a) Injection, fuel-oxidant-fuel; stable combustion. ⟷ 0.1 in. (2.54 mm)

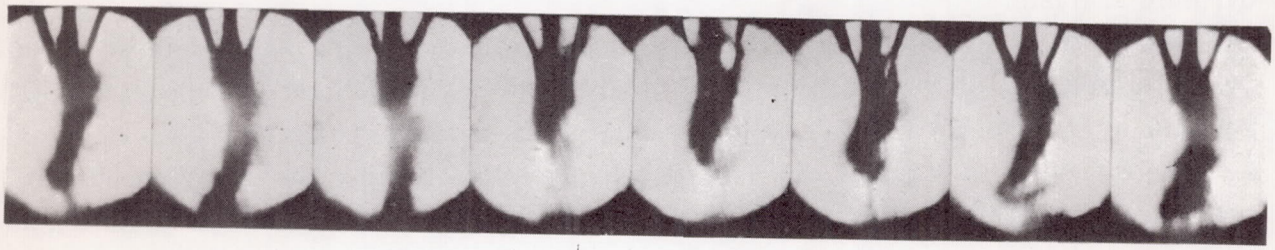

(b) Injection, fuel-oxidant-fuel; self-coupled oscillation.

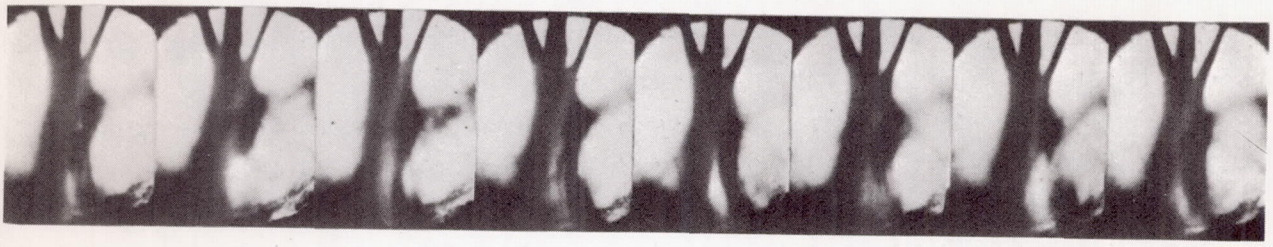

(c) Injection, oxidant-fuel-oxidant; stable combustion.

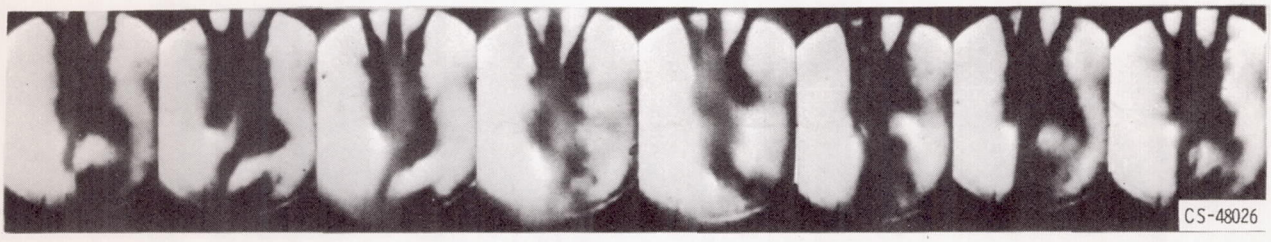

(d) Injection, oxidant-fuel-oxidant; self-coupled oscillation.

Figure 4. - Impinging jet behavior with first transverse mode instability. Mixed oxides of nitrogen and hydrazine propellant combination.

The tests with the two-dimensional combustor emphasize the need for an analytical description of liquid jet dynamics. The experimental tests provide only qualitative descriptions with perturbations in mass release rate, the crucial quantity for instability, being most elusive. The physical insight gained from such tests, however, is valuable in formulating an analytical model of jet dynamics.

LIQUID JET ATOMIZATION MODEL

In the tests with the two-dimensional circular combustor, the transverse acoustic particle velocity exhibited a dominant effect on the breakup of the liquid jet. The effect of a transverse flow of gas on jet breakup, therefore, is of particular concern in any dynamic analysis.

The effect of a steady transverse flow of gas on the breakup of water jets was studied by Clark (ref. 9). In that study, an analytical model was formulated to support the experimental effect of steady flow on jet breakup. The model is particularly useful in examining the dynamic behavior of a jet. It conveniently describes the instantaneous jet properties during breakup and is not restricted to integral properties such as jet length or breakup time as are some other models (which restrict their dynamic implications).

Figure 5 illustrates the model formulated in reference 9 for the basic mechanism of breakup of a liquid jet element in a cross flow of gas. The mechanism is similar to that used and observed for drop breakup in reference 11.

The external pressure distribution creates a pressure gradient within a element of liquid jet which flattens the liquid element. At the edges of this flattened element drops and ligaments are torn off by the combined action of the tangential stress and surface tension. Breakup of this type is restricted to conditions where external forces are large compared with surface forces.

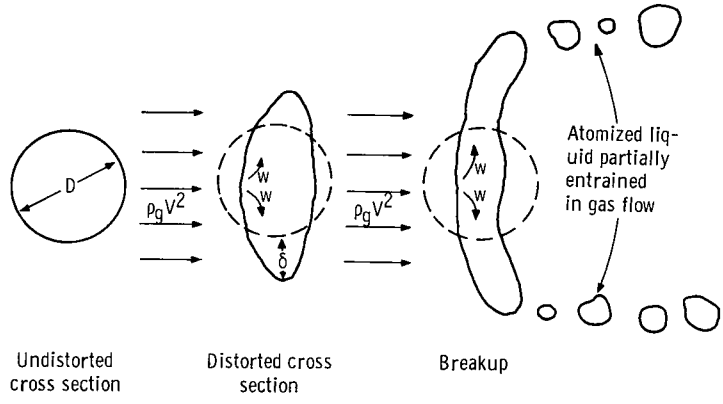

Figure 5. - Basic mechanism of liquid jet element breakup (ref. 9).

The distortion δ of an element of jet caused by an acceleration a persisting for a period τ from the time of injection $t - \tau$ is given by

$$\delta = \int_{t-\tau}^{t} \int_{t-\tau}^{t^x} a \, dt^{xx} \, dt^x \tag{1}$$

The acceleration is caused by the external forces acting on the element of liquid mass. From a consideration of the pressure distribution around the cylindrical element, the acceleration becomes

$$a = 2 \frac{\rho_g}{\rho_l} \frac{V^2}{D} \tag{2}$$

Breakup occurs when the distortion relative to the element diameter $\epsilon = \delta/D$ attains some critical value. The basic mechanism for breakup, therefore, is defined by

$$\epsilon = \frac{2}{\rho_l D^2} \int_{t-\tau}^{t} \int_{t-\tau}^{t^x} \rho_g V^2 \, dt^{xx} \, dt^x \tag{3}$$

For a steady flow of gas the breakup time τ_{ss} given by the integration of equation (3) is

$$\tau_{ss} = \frac{D}{V} \left(\frac{\rho_l}{\rho_g} \epsilon \right)^{1/2} \tag{4}$$

Steady flow experiments with water jets showed that an ϵ of 3 to 4.5 characterized a mean breakup time τ_{ss} where only 50 percent of the jet element mass remains intact. Complete breakup was characterized by an ϵ of 10 to 15.

The study of Clark revealed other properties that are useful in the dynamic analysis of jet breakup. Although equation (3) describes the basic mechanism, the actual breakup process exhibited distributed properties that are not implied by the equation. In particular, the breakup of a jet did not occur after a discrete time τ from injection as implied by equation (3). Rather, breakup or mass removal occurred over some finite time or along some finite length of jet. On the average, the measured distribution of the mass release rate as determined from figure 17 of reference 9 was distributed with time or length as shown in figure 6. These distributed properties will be considered in the dy-

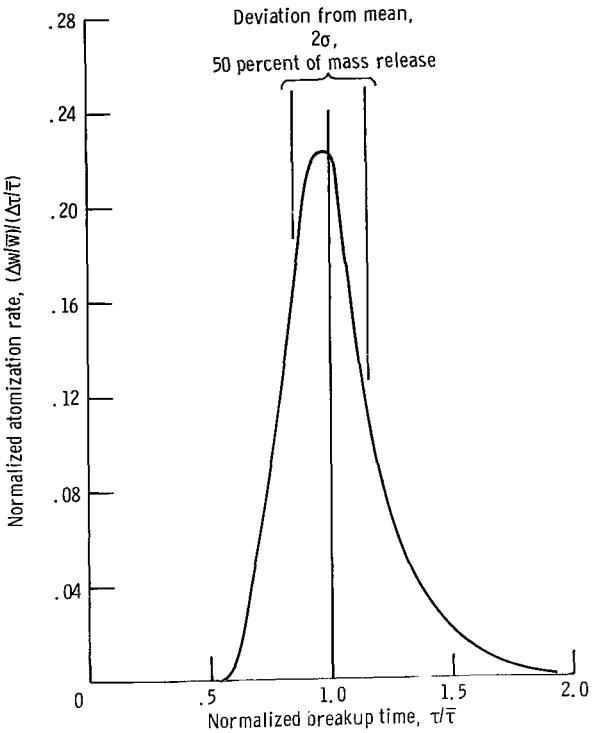

Figure 6. - Distributed properties of jet atomization.

namic analysis. Initially, however, the discrete breakup mechanism given by equation (3) will be examined for dominant dynamic properties. The effect of the distributed nature of breakup on dynamics will be examined separately.

The study by Clark also showed that the velocity V should be the gas velocity relative to the liquid element. Expanding this concept to an axial jet in a cylinder, the magnitude of the relative velocity vector acting on an element of jet is given by

$$V = \left(\left| u_\ell - u_z \right|^2 + u_\theta^2 + u_r^2 \right)^{1/2} \tag{5}$$

This definition of the effective velocity changes the concept of simple element flattening previously conveyed. Rather, jet distortion involves a more complex motion of liquid mass caused by cummulative momentum transfer from the gases independent of the direction of the applied force. Clark's experiments, although not complete, verified a breakup time independent of force direction. Proceeding with this concept, the basic mechanism for jet distortion caused by transverse acoustic oscillations, where u_θ, u_r,

and ρ_g are time varying quantities, becomes

$$\epsilon = \frac{2}{\rho_l D^2} \int_{t-\tau}^{t} \int_{t-\tau}^{t^x} f(t^{xx}) dt^{xx}\, dt^x \tag{6}$$

where

$$f(t) = \rho_g(t) \left[\left| u_l - u_z \right|^2 + u_\theta^2(t) + u_r^2(t) \right] \tag{7}$$

Equation (6) is the analytical expression of the breakup mechanism used herein to examine the dynamic properties of liquid jet atomization. Dynamic properties are primarily established by the time dependent aspects of equation (6). For comparison, the approach of Buffum and Williams (ref. 12) for the analysis of jet deflection would give an expression with similar time dependent properties when breakup is characterized by a critical value of jet deflection.

THEORETICAL ANALYSIS

Analytical expressions based on certain simplifying assumptions required for closed-form solutions will be derived for the dynamic response of jet atomization in a transverse acoustic mode.

The atomization rate w' for a jet with a discrete breakup time τ and a constant velocity is given by

$$w'(t) = -\frac{d\tau}{dt} \tag{8}$$

An expression for $d\tau/dt$ for jet breakup in an acoustic field is obtained from a consideration of equation (6). In a time varying environment, each element of jet experiences a different time history of applied forces. If the criterion of a nonvarying critical distortion ϵ for all elements is applied, the following must be satisfied

$$\frac{d\epsilon}{dt} = 0 = \frac{2}{\rho_l D^2} \int_{t-\tau}^{t} \int_{t-\tau}^{t^x} f(t^{xx}) dt^{xx}\, dt^x \tag{9}$$

Applying the Leibnitz rule for differentiation of an integral results in this expression of equation (9):

$$\int_{t-\tau}^{t} \frac{\delta}{\delta t} \int_{t-\tau}^{t^x} f(t^{xx})dt^{xx}\, dt^x + \int_{t-\tau}^{t} f(t)dt = 0 \tag{10}$$

Reapplying the Leibnitz rule to the first term of equation (10) gives the expression

$$-\left(1 - \frac{d\tau}{dt}\right) f(t - \tau) \int_{t-\tau}^{t} dt + \int_{t-\tau}^{t} f(t)dt = 0 \tag{11}$$

or

$$-\tau\left(1 - \frac{d\tau}{dt}\right) f(t - \tau) + \int_{t-\tau}^{t} f(t)dt = 0 \tag{12}$$

Solving for $-d\tau/dt$ gives the atomization rate w' as

$$w' = -\frac{d\tau}{dt} = \frac{\int_{t-\tau}^{t} f(t)dt}{\tau f(t - \tau)} - 1 \tag{13}$$

The function $f(t)$ depends on specific properties of an acoustic mode at the location of the jet. Equation (7) uses a conventional expression for the velocity components. For convenience in analyzing the general case of transverse acoustic modes, however, a different notation will be used. The transverse velocity will be resolved into two phase-related components. These are the in-phase u_R and the 90^o out-of-phase u_I components with respect to the time variations in pressure. These components can be readily identified from the usual first-order solutions for acoustic modes. In this notation the function $f(t)$ is given by

$$f(t) = \rho_g\left(|u_l - u_z|^2 + u_R^2 + u_I^2\right) \tag{14}$$

For any of the transverse modes, the pressure, density, and velocities are of the form

$$P(t) = \overline{P}(1 + \hat{P}' \cos \omega t) \tag{15}$$

$$\rho_g(t) = \overline{\rho}_g\left(1 + \frac{1}{\gamma}\hat{P}' \cos \omega t\right) \tag{16}$$

$$u_R(t) = \hat{u}_R \cos \omega t \tag{17}$$

$$u_I(t) = \hat{u}_I \sin \omega t \tag{18}$$

Using these properties, the function f(t) expressed as a harmonic series becomes

$$f(t) = \overline{\rho}_g\left[\left(|u_\ell - u_z|^2 + \frac{1}{2}\hat{u}_R^2 + \frac{1}{2}\hat{u}_I^2\right) + \frac{1}{\gamma}\hat{P}'\left(|u_\ell - u_z|^2 + \frac{3}{4}\hat{u}_R^2 + \frac{1}{4}\hat{u}_I^2\right)\cos \omega t\right.$$

$$\left. + \frac{1}{2}\left(\hat{u}_R^2 - \hat{u}_I^2\right)\cos 2\omega t + \frac{1}{4\gamma}\hat{P}'\left(\hat{u}_R^2 - \hat{u}_I^2\right)\cos 3\omega t\right] \tag{19}$$

Neglecting the higher harmonic terms, the function takes the form

$$f(t) = \overline{\rho}_g V_{rms}^2\left(1 + \hat{V}'\frac{\hat{P}'}{\gamma}\cos \omega t\right) \tag{20}$$

where

$$\hat{V}' = \frac{|u_\ell - u_z|^2 + \frac{3}{4}\hat{u}_R^2 + \frac{1}{4}\hat{u}_I^2}{|u_\ell - u_z|^2 + \frac{1}{2}\hat{u}_R^2 + \frac{1}{2}\hat{u}_I^2} \tag{21}$$

and

$$V_{rms}^2 = |u_\ell - u_z|^2 + \frac{1}{2}\hat{u}_R^2 + \frac{1}{2}\hat{u}_I^2 \tag{22}$$

Performing the integration indicated in equation (13) with equation (20) as the forcing function results in the solution obtained by assuming that the difference between τ and $\overline{\tau}$ is small:

$$w'(t) = \hat{V}' \frac{\hat{P}'}{\gamma} \left[\frac{\frac{1}{\omega\bar{\tau}} \sin \omega t - \frac{1}{\omega\bar{\tau}} \sin \omega(t - \bar{\tau}) - \cos \omega(t - \bar{\tau})}{1 + \hat{V}' \frac{\hat{P}'}{\gamma} \cos \omega(t - \bar{\tau})} \right] \tag{23}$$

Figure 7 shows several examples of the atomization rate perturbations given by equation (23) for several values of $\omega\bar{\tau}$. Although the atomization rate oscillations are not pure harmonic functions, they show a change in phase angle and amplitude relation between pressure and atomization rate with a change in breakup time.

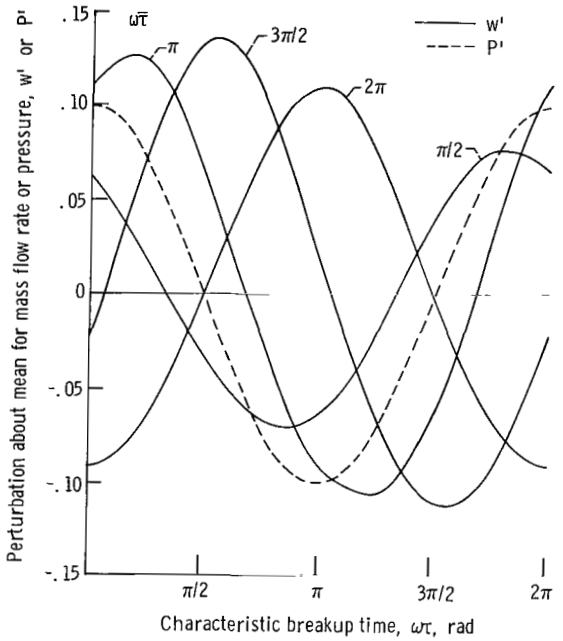

Figure 7. - Effect of mean breakup time on atomization rate perturbations for amplitude parameter, $(\hat{V}'/\gamma)\hat{P}'$, of 0.1.

One method of examining such dynamic behavior is to extract two response factors: the in-phase N_R and out-of-phase N_I components of the atomization rate with respect to pressure. Since the pressure oscillation was assumed a cosine function, the first-order terms for the atomization rate are given by

$$w'(t) = \hat{P}'(N_R \cos \omega t + N_I \sin \omega t) \tag{24}$$

where the response factors are given by

$$N_R = \frac{1}{\pi(\hat{P}')^2} \int_0^{2\pi} w'(t)\hat{P}' \cos \omega t \, d\omega t \tag{25}$$

and

$$N_I = \frac{1}{\pi(\hat{P}')^2} \int_0^{2\pi} w'(t)\hat{P}' \sin \omega t \, d\omega t \tag{26}$$

An alternate expression for the first-order expression is

$$w'(t) = \hat{w}' \cos \omega(t + \theta) \tag{27}$$

where the gain and angle are defined by

$$\left.\begin{aligned} \frac{\hat{w}'}{\hat{P}'} &= \left(N_R^2 + N_I^2\right)^{1/2} \\ \theta &= \tan^{-1} \frac{N_I}{N_R} \end{aligned}\right\} \tag{28}$$

In either of these notations, N_R and N_I represent the real and imaginary part of a type of admittance relating atomization rate and pressure.

Using the atomization rate given by equation (23), the integral equation (25) and (26) define N_R and N_I for jet atomization in a transverse acoustic mode. Although no exact analytical solution exists for these integrals, an expansion to first order in $\hat{P}'$ gives the result,

$$N_R = \frac{\hat{V}'}{\gamma}\left(\frac{\sin \omega\bar{\tau}}{\omega\bar{\tau}} - \cos \omega\bar{\tau}\right) \tag{29}$$

and

$$N_I = \frac{\hat{V}'}{\gamma}\left[\left(\frac{1 - \cos \omega\bar{\tau}}{\omega\bar{\tau}}\right) - \sin \omega\bar{\tau}\right] \tag{30}$$

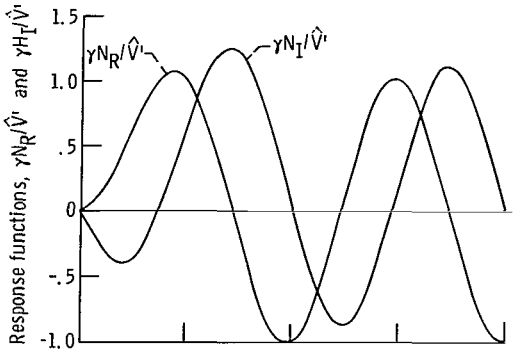

(a) Response factors.

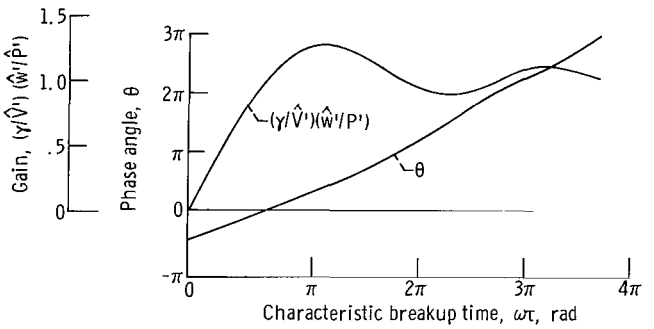

(b) Gain and phase angle.

Figure 8. - Dynamic properties of jet atomization process from theoretical analysis.

Figure 8 shows the dynamic properties of the atomization process given by these solutions. Both N_R and N_I are periodic with $\omega\overline{\tau}$ and exhibit extreme values of about $\pm(\hat{V}'/\gamma)$ (fig. 8(a)). In general when either N_R or N_I is a maximum or minimum, the other is approximately equal to zero. Conditions at $\omega\overline{\tau}$ near zero are an exception. In this region, the gain, $\hat{w}'/\hat{P}'$, decreases with $\omega\overline{\tau}$ (fig. 8(b)) and causes both N_R and N_I to approach zero. When $\omega\overline{\tau}$ is greater than π, the gain is relatively constant but the phase angle θ increases nearly linearly with $\omega\overline{\tau}$.

The response factors N_R and N_I are useful boundary conditions representing the combustion process in a stability analysis of a combustor (ref. 13). The quantitative significance of these properties on stability can only be established from a system analysis that mates combustion properties with system acoustics. Qualitatively, the component of the atomization rate in phase with the pressure oscillation N_R is of deciding importance in many instances. It is of primary importance in the phenomenological approach to combustion instability. If the magnitude of N_R of a process approaches unity, the contribution of the process to unstable operation is substantial.

The magnitude of N_R for the atomization process can fall in the critical region

near unity. The maximum value of N_R is about $\hat{V}'/\gamma$, where $\hat{V}'$ is given by equation (21). The maximum value of N_R for the condition of an axial velocity difference alone (u_R and $u_I = 0$) is $1/\gamma$. For u_R alone, $(N_R)_{max}$ is $\frac{3}{2}\gamma$; for u_I alone, $(N_R)_{max}$ is $\frac{1}{2}\gamma$. These values are near unity and indicate that the jet atomization process can be an important dynamic component of a combustion system.

In addition to these effects of acoustic velocities on the magnitude of the response factors, the mean breakup time of the jet is also velocity sensitive. This can be shown by considering only the first harmonic content of f(t) given by equation (20) and performing the integration indicated by equation (6). The limiting solution as $\omega\bar{\tau}$ becomes large is

$$\omega\bar{\tau} = \left(\frac{D}{V_{rms}}\omega\right)\left(\frac{\rho_l}{\rho_g}\epsilon\right)^{1/2} \tag{31}$$

This form of the solution is identical to that used by Clark for a steady flow (eq. (5)). Acoustic affects enter into the definition of the velocity term V_{rms} given by equation (22). The effect of velocity perturbations on mean breakup time is shown in figure 9.

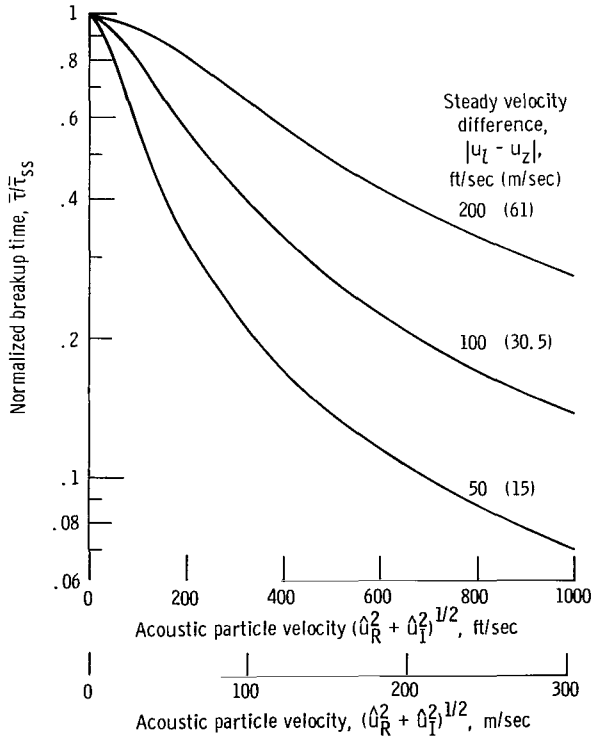

Figure 9. - Effect of acoustic velocity oscillations on mean breakup time.

An increase in velocity perturbations decreases the breakup time below its steady-state value. The effect decreases with an increase in $|u_l - u_z|$.

NUMERICAL ANALYSIS

The theoretically derived dynamic properties of jet atomization involved a number of simplifying assumptions of unknown quantitative significance. In general, the procedures resulted in analytical limitations similar to those restricting linear analysis to small perturbations. An important application of jet dynamics, however, is in the region of finite and large acoustic oscillations. These uncertainties of the analytical procedures prompted a numerical analysis which preserved all nonlinear behavior of the assumed mechanism of atomization. An analysis based on the following procedure was programmed for a digital computer to quantitatively establish nonlinear dynamic properties for some representative acoustic conditions.

The basic breakup mechanism described by equation (6) and the general description of f(t) for a transverse acoustic mode given by equation (19) were assumed. An exact integration of equation (6) between the time of injection $t_0 = t - \tau$ and the time t was performed for these acoustic properties. The solution which defines the distortion of any element of jet is given by

$$\left(\frac{D}{V_{rms}}\omega\right)^2 \frac{\rho_l}{\rho_g}\epsilon = \omega^2(t - t_0)^2 + 2\frac{\hat{P}'}{\gamma}\hat{V}'\left[\cos\omega t_0 - \cos\omega t - \omega(t - t_0)\sin\omega t_0\right]$$

$$+ \frac{1}{4}\frac{\left(\hat{u}_R^2 - \hat{u}_I^2\right)}{\left(V_{rms}\right)^2}\left[\cos 2\omega t_0 - \cos 2\omega t - 2\omega(t - t_0)\sin 2\omega t_0\right]$$

$$+ \frac{1}{18}\frac{\hat{P}'}{\gamma}\frac{\left(\hat{u}_R^2 - \hat{u}_I^2\right)}{\left(V_{rms}\right)^2}\left[\cos 3\omega t_0 - \cos 3\omega t - 3\omega(t - t_0)\sin 3\omega t_0\right] \qquad (32)$$

where V_{rms} and $\hat{V}'$ are defined as previously in equations (21) and (24).

On specifying acoustic properties for a particular mode, tables of values relating $\left[(D/V_{rms})\omega\right]^2(\rho_l/\bar{\rho}_g)\epsilon$ to ωt can be generated for progressive incremental values of ωt_0 encompassing one cycle of oscillation. The breakup criterion specifies that any element will breakup when ϵ and, therefore, $\left[(D/V_{rms})\omega\right]^2(\rho_l/\bar{\rho}_g)\epsilon$ reaches some con-

stant value. On specifying a specific value of this modified distortion parameter, a search of the tables will give interpolated values of ωt which satisfy the breakup criterion for progressive values of ωt_0. The difference $\omega t - \omega t_0$ is the dimensionless breakup time $\omega\tau$ for successive jet elements. From such results, the atomization rate w'(t) is given by the incremental change $-(\Delta\omega\tau/\Delta\omega t)$ as indicated by equation (8). These values of w'(t) used in a numerical integration of equations (25) and (26) give the in-phase N_R and out-of-phase N_I response factors. A value of $\omega\bar{\tau}$ characterizing a selected value of the modified distortion parameter is established by a numerical average of $\omega\tau$ for the elements contained within one cycle of oscillation.

In the actual procedure, tables of modified distortion parameters for time increments of 1000 per cycle were computed for 100 values of initial time.

APPLICATION TO SPECIFIC MODES

A general description for acoustic properties was used in the development of the theoretical and numerical analysis of jet atomization. Application of these analysis to several specific conditions of acoustic resonance will illustrate some of the important effects of variable acoustic properties on jet dynamics. Three transverse acoustic modes will be considered. These are the first or lowest order traveling, standing, and radial modes.

Traveling Transverse Acoustic Modes

The first-order terms for the properties of a traveling mode are given by

$$P = \bar{P}\left[1 + A\gamma J_1(\alpha)\cos(\omega t + \theta)\right] \tag{33}$$

$$\rho_g = \bar{\rho}_g\left[1 + AJ_1(\alpha)\cos(\omega t + \theta)\right] \tag{34}$$

$$u_\theta = Ac\,\frac{J_1(\alpha)}{\alpha}\cos(\omega t + \theta) \tag{35}$$

$$u_r = Ac\left[J_0(\alpha) - \frac{J_1(\alpha)}{\alpha}\right]\sin(\omega t + \theta) \tag{36}$$

where $\alpha = 1.841\ r$.

These properties establish the following identities for the notation used in the general description of a transverse mode in equations (15) to (18).

$$\left.\begin{aligned} u_\theta &= u_R \\ u_r &= u_I \\ \hat{P}' &= A\gamma J_1(\alpha) \\ u_R &= \frac{C\hat{P}'}{\alpha\gamma} \\ u_I &= \frac{C\hat{P}'}{\alpha\gamma}\left[\alpha \frac{J_0(\alpha)}{J_1(\alpha)} - 1\right] \end{aligned}\right\} \tag{37}$$

The principal features of this traveling mode with regard to jet breakup are that (1) pressure and density perturbations are a maximum at the wall and decrease to zero at the center, (2) tangential velocity perturbations u_θ are about 1.5 times larger at the center than at the wall, and (3) radial velocity perturbations u_r are zero at the wall but equal the u_θ perturbations at the center. The consequences of combining equal u_θ and u_r perturbations at the center is a rotating velocity vector of constant magnitude with no velocity perturbations. On approaching the wall, the steady component of this velocity vector decreases, and the perturbating component increases until it is entirely a perturbating component at the wall. This behavior is independent of the angular position. The effect of such acoustic properties on the jet dynamics can be shown by a parametric survey of some of the variables.

Effect of steady velocity difference and pressure amplitude at wall position. - At a wall position where velocity perturbations are in-phase and proportional to the pressure perturbations, the acoustic properties are similar to those of a traveling plane wave. The analytical and numerical results of the jet response at this position are shown in figure 10 for a pressure amplitude $\hat{P}'$ of 0.1 and several values of the steady velocity difference $|u_l - u_z|$. The numerical results show the same periodic variation of the response factors with $\omega\bar{\tau}$ previously described for the analytical results. Quantitatively, however, the results of the two analyses differ.

The maximum peak value of N_R (fig. 10(a)), obtained when $|u_l - u_z|$ is zero for both analysis, equals 1.32 analytically and 1.58 numerically. The separation between the analytical and numerical peaks with respect to $\omega\bar{\tau}$ also suggests a nonlinear velocity effect on jet breakup time. The numerical N_I curves (fig. 10(b)) show an increase over the analytical results comparable to that for N_R. For the constant $\hat{P}'$ conditions of

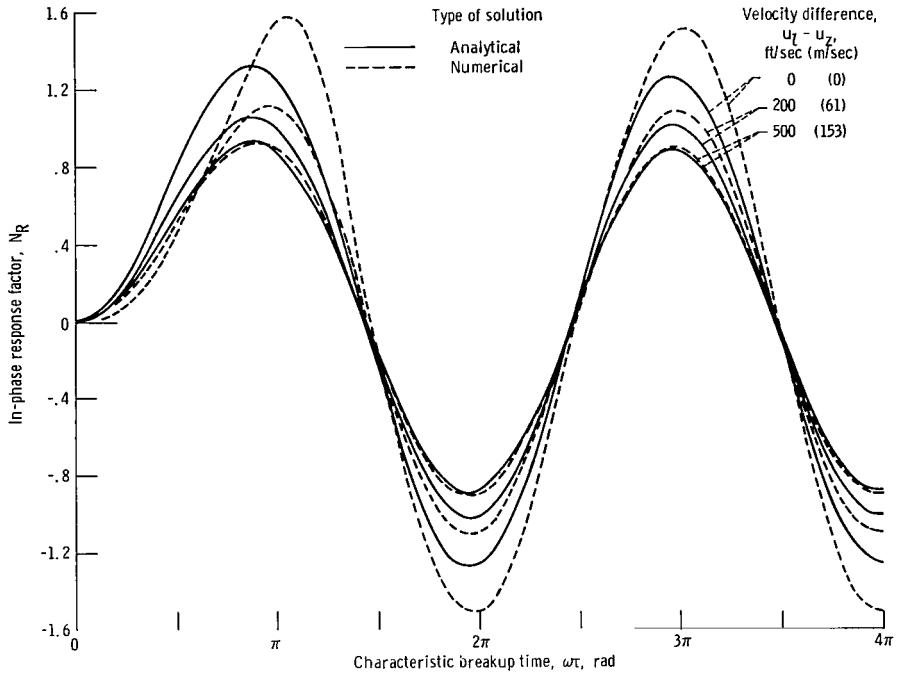

(a) In-phase response factor; real gain (w'/P').

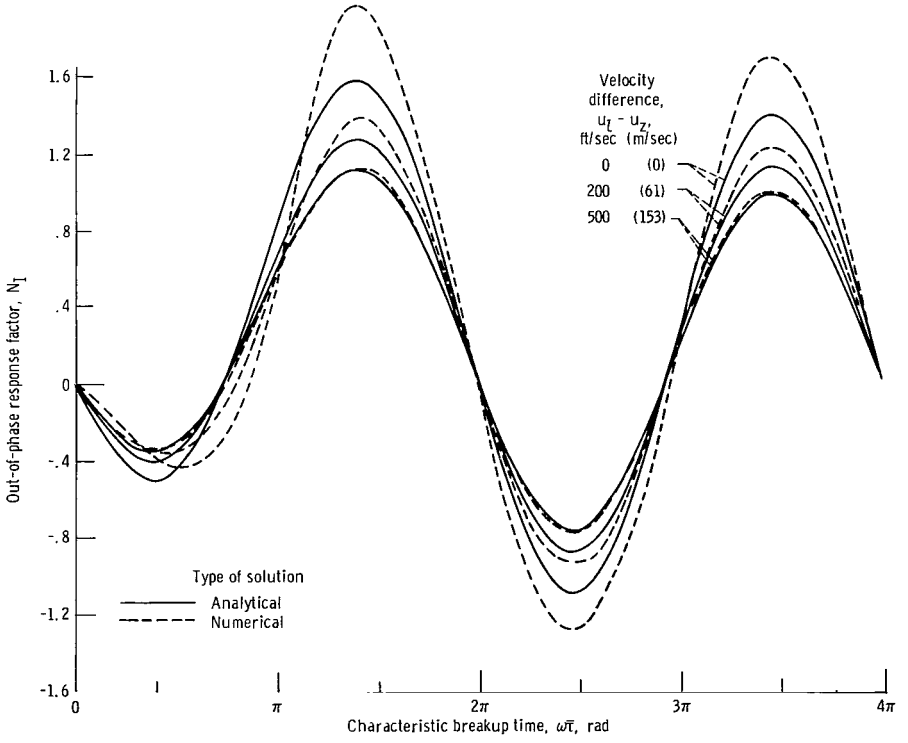

(b) Out-of-phase response; imaginary gain (w'/P').

Figure 10. - Response at wall position of traveling mode. Maximum pressure amplitude, 0.1; ratio of specific heats, 1.2; speed of sound, 5000 feet per second (1520 m/sec).

figure 10, the peak values decrease with an increase in $|u_l - u_z|$ and the difference between the results of the two analyses decreases.

The effect of both $|u_l - u_z|$ and $\hat{P}'$ on peak response is shown in figure 11. The peak values of N_R near an $\omega\bar{\tau}$ of 3π are used for the comparison. When $|u_l - u_z|$ is finite and constant, the response factor has an asymptotic minimum at low amplitudes. At high amplitudes, the analytical results approach a maximum asymptotically; however, the numerical result is more complex. As $|u_l - u_z|$ increases, pressure amplitude for the transition between these two asymptotic limits also increases. The minimum asymptote for the numerical results equals the analytical value of $1/\gamma$. The analytical value of $1/\gamma$ is the pressure sensitive response of the process when velocity oscillations are zero. The properties of the N_I response factor are similar to those N_R characteristics.

These results empahsize the importance of the in-phase velocity perturbation u_R on the response of the jet atomization process. The magnitude of u_R is proportional to

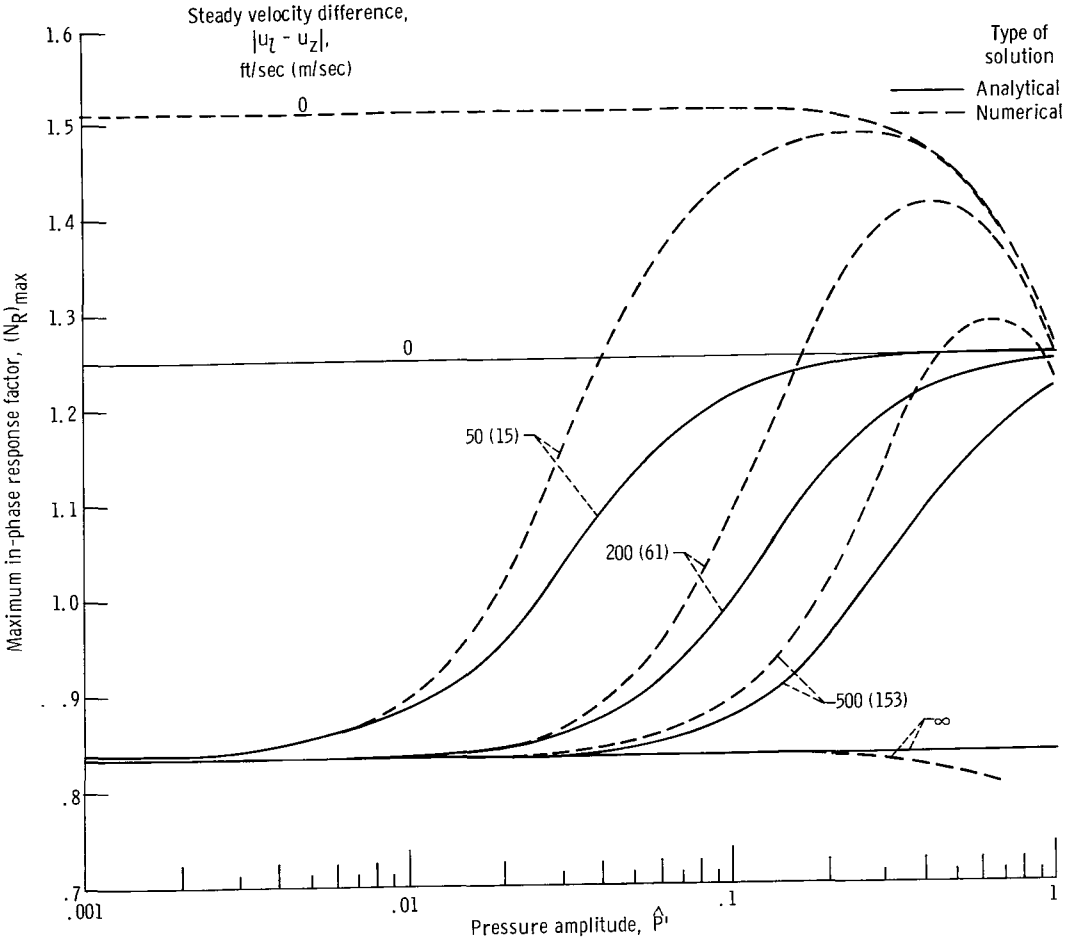

Figure 11. - Maximum in-phase response factor at wall position of traveling mode. Ratio of specific heats, 1.2; speed of sound, 5000 feet per second (1520 m/sec). Maximum values near $\omega\bar{\tau} = 3\pi$ radians used for comparison.

P'. At high amplitudes u_R dominates $|u_l - u_z|$ and the response is significantly larger than for a dominating $|u_l - u_z|$. In the case of the numerical results, emphasizing u_R can almost double the response. A strong traveling wave or a low velocity difference environment, therefore, can cause a large dynamic response from the jet atomization process.

The quantitative difference between the numerical and analytical results for a dominating in-phase velocity perturbation is caused by the nonlinear effects preserved in the numerical procedures. This nonlinear behavior is clearly evident in the cyclic variation in breakup time and atomization rate with time shown in figure 12. Two abrupt changes

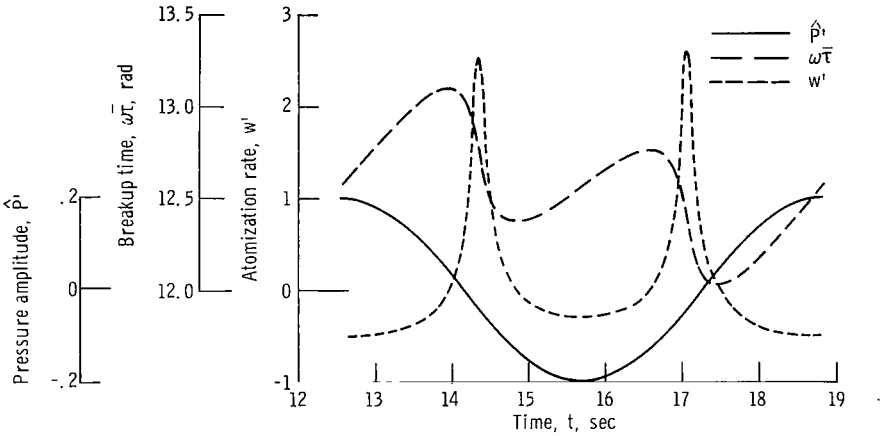

Figure 12. - Typical numerical solution for jet breakup time and atomization rate variations with time for pressure amplitude of 0.2. Steady velocity difference, 200 feet per second (61 m/sec); ratio of specific heats, 1.2; speed of sound, 5000 feet per second (1520 m/sec); maximum angular velocity, 452.7 feet per second (138 m/sec).

occur for each cycle of pressure oscillation. These are caused by the velocity perturbation. Both the positive and negative velocity peaks of the velocity perturbation enhance the breakup process. This dynamic behavior is characterized by N_R and N_I, which express only the first harmonic content of the atomization rate perturbations. In figure 12 the first harmonic content of the highly nonlinear atomization rate is obscure. In contrast, very small nonlinear effects were evident in the analytical atomization rate (fig. 7) where only the first harmonic content of the areodynamic forces on the jet were considered. Preserving the nonlinear content of these forces and eliminating other assumptions in the analytical procedures contribute to additional first-order content of the atomization rate perturbations.

As previously shown in figure 9, velocity perturbations also affect the mean breakup time $\omega\bar{\tau}$. Figure 13 shows $\omega\bar{\tau}$ properties at the wall position in the traveling mode.

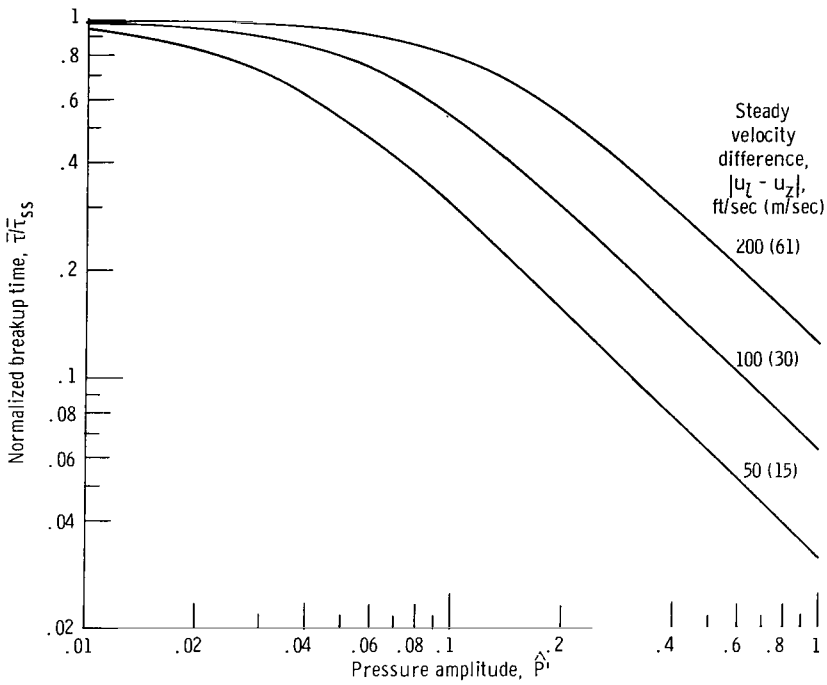

Figure 13. - Analytical normalized breakup time at wall position of traveling mode. Ratio of specific heats, 1.2; speed of sound, 5000 feet per second (1520 m/sec).

As the pressure amplitude becomes large, substantial decreases in breakup time are predicted. The numerical solutions give comparable changes. Such changes in $\omega\bar{\tau}$ cause significant changes in the response factors with amplitude because N_R and N_I are periodically related to $\omega\bar{\tau}$.

This nonlinear effect of pressure amplitude on $\omega\bar{\tau}$ introduces the possibility of nonlinear instability limits for a rocket combustor. Referring to figure 8, a combustor with atomization limited combustion may be stable in an $\omega\bar{\tau}$ region near 2π radians, where N_R is negative. Velocity perturbation introduced by a bomb or other disturbance could reduce $\omega\bar{\tau}$ to a region where N_R is sufficiently high to overcome acoustic losses and cause instability. If the disturbance were sufficiently large to reduce $\omega\bar{\tau}$ to near zero where N_R is small, instability could occur during the decay of the disturbance. During decay ($\omega\bar{\tau}$ increasing), the magnitude of N_R increases. Therefore, if the peak response is larger than the acoustic losses, there should be some size of disturbance above which the combustor is always unstable.

Effect of radial position. - The magnitude of the steady and perturbating content of the transverse velocity vector varies with radial position. The effect of such changes on breakup time cause the most significant changes in the response factors. Figure 14 shows the change in breakup time with radial position. Breakup time (and jet length which is proportional to $\bar{\tau}$) decrease on approaching the center. The fractional change decreases with an increase in $|u_l - u_z|$.

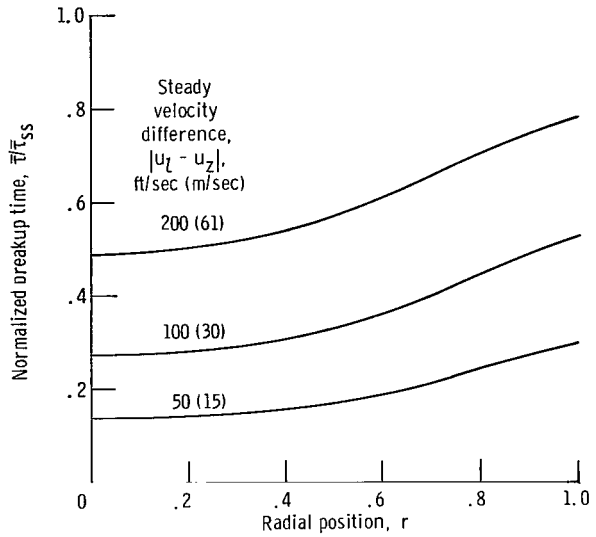

Figure 14. - Analytical variation in normalized breakup time with radial position in traveling mode. Pressure amplitude, 0.1 at radial position, 1.0; ratio of specific heats, 1.2; and speed of sound, 5000 feet per second (1520 m/sec).

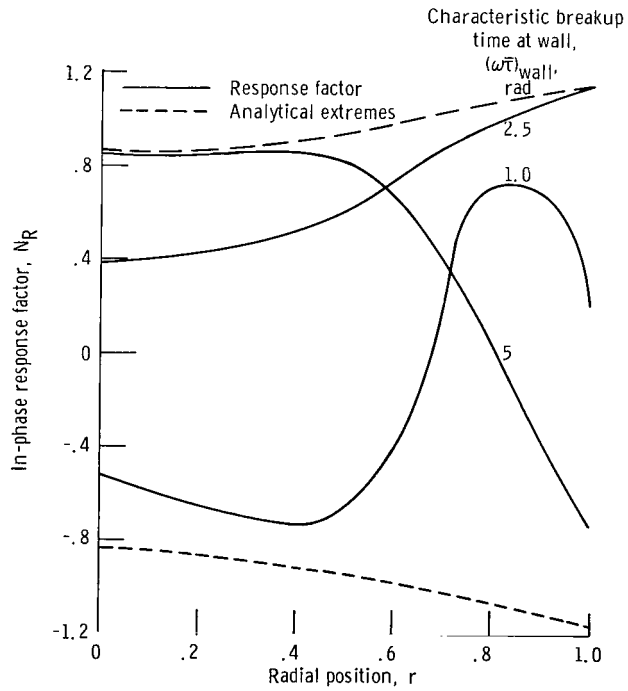

Figure 15. - Variation in in-phase response factor with radial position in traveling mode. Pressure amplitude, 0.1 at radial position, 1.0; and steady velocity difference, 100 feet per second (30 m/sec).

It has been previously shown that the response factors N_R and N_I vary periodically with $\omega\bar{\tau}$. Substantial changes in these response factors with radial position, therefore, can be expected from changes in $\bar{\tau}$ with position. In fact, the response factors can exhibit periodic variations with radial position. Examples for several jet conditions are shown in figure 15. The value of N_R can be positive at the wall and negative at the center, the converse, and many intermediate conditions. The values of N_I vary in a similar manner. Such changes in response with radial position imply that the manner in which jets are distributed within the cross-sectional area would significantly affect the average response.

The dynamic behavior with radial position can deviate considerably from the examples shown in figure 15. The variations of response with radial position, however, are contained within limiting values as indicated in figure 15. The limiting values at the wall are those previously discussed where low values of $|u_l - u_z|$ increase the limiting value. At the center the limiting value is $1/\gamma$, the pressure sensitive value, for all conditions.

The varied characteristics of the response factors with radial position preculdes any general characterization of the behavior. Only in the case of high axial velocity differences or low pressure amplitudes is the response relatively uniform throughout.

Standing Transverse Acoustic Mode

The first-order terms for the properties of the standing mode are given by

$$P = \bar{P}\left[1 + A\gamma J_1(\alpha)\cos\ \omega t\ \cos\ \theta\right] \tag{38}$$

$$\rho_g = \bar{\rho}_g\left[1 + AJ_1(\alpha)\cos\ \omega t\ \cos\ \theta\right] \tag{39}$$

$$u_\theta = Ac\ \frac{J_1(\alpha)}{\alpha}\ \sin\ \omega t\ \sin\ \theta \tag{40}$$

$$u_r = Ac\left[J_0(\alpha) - \frac{J_1(\alpha)}{\alpha}\right]\sin\ \omega t\ \sin\ \theta \tag{41}$$

In the standing mode both u_θ and u_r are out-of-phase with the pressure so that

$$u_I = \left(u_\theta^2 + u_r^2\right)^{1/2} \tag{42}$$

and the following identities are established with regard to equations (15) to (18)

$$\left.\begin{aligned} \hat{P}' &= A\gamma J_1(\alpha)\cos\theta \\ u_I &= \frac{cP'}{\gamma\alpha}\tan\theta\left\{2 + \left[\alpha\frac{J_0(\alpha)}{J_1(\alpha)}\right]^2 - 2\left[\alpha\frac{J_0(\alpha)}{J_1(\alpha)}\right]\right\}^{1/2} \\ \alpha &= 1.841\ r \end{aligned}\right\} \tag{43}$$

In the standing mode, a pressure node exists along a diametrical path of $\theta = \pi/2$. Along the path of $\theta = 0$ the angular velocity is zero or at a nodal condition. As implied by these nodes, the standing mode differs from the traveling mode in that acoustic properties vary with angular position as well as radial position. With regard to jet dynamics, however, complexity is somewhat reduced because velocity perturbations are restricted to out-of-phase perturbations that can only vary in amplitude between the limits $\pm(c/\alpha)(\hat{P}'_{\theta=0}/\gamma)$.

The wall position at the angular velocity node ($\theta = 0$) is unique with regard to jet dynamics because velocity perturbations disappear and the density oscillations alone cause perturbations in the forces acting on the jet. This condition was studied in reference 14. In the analytical expressions for the response factors (eqs. (29) and (30)), the parameter $\hat{V}'$ is equal to one and is independent of the steady axial velocity difference and the pressure amplitude. The maximum values of N_R and N_I, therefore, are equal to about $1/\gamma$.

Numerical and analytical solutions for N_R are compared in figure 16. Nonlinear effects preserved in the numerical analysis appear to have a small effect on response in that agreement with the analytical solution is good even at high amplitudes. Similar agreement is obtained for N_I. Jet response to density oscillations alone, therefore, give a maximum value of about $1/\gamma$ for the response factors. The result would be identical for a velocity node position in a longitudinal or any other mode.

At any other position within the standing mode, the maximum values of N_R and N_I are affected by velocity perturbations restricted to out-of-phase properties. The effect of an out-of-phase velocity is shown in figure 17. Analytical and numerical solutions for N_R are compared for $|u_\ell - u_z| = 0$ at a quarter wave position ($\theta = \pi/4$) at the wall. At $\omega\bar{\tau} = 3\pi$ radians, the maximum analytical response is $1/2\gamma$ (0.417) or 1/2 the pressure sensitive value at these dominating out-of-phase velocity conditions. The numerical solution shows a maximum response of only 0.338 at near 3π radians. This shows that an out-of-phase velocity depresses the response, and it was previously shown that an in-phase velocity enhanced the response. It can be concluded that a u_I velocity has

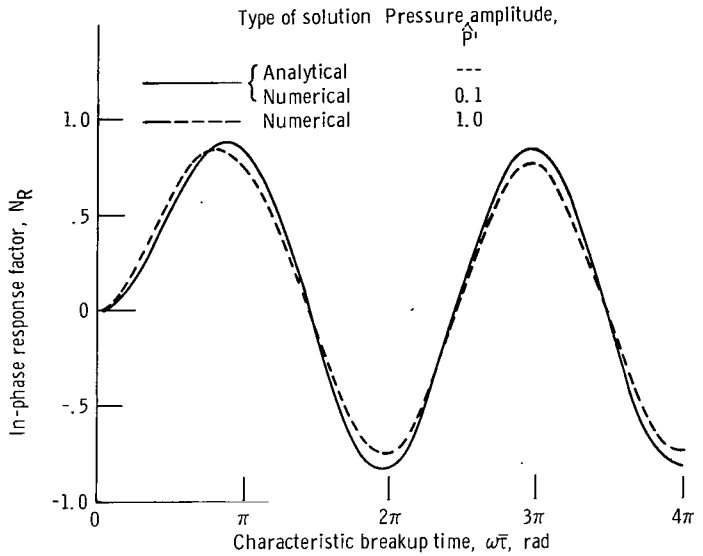

Figure 16. - Response at velocity node in standing mode.

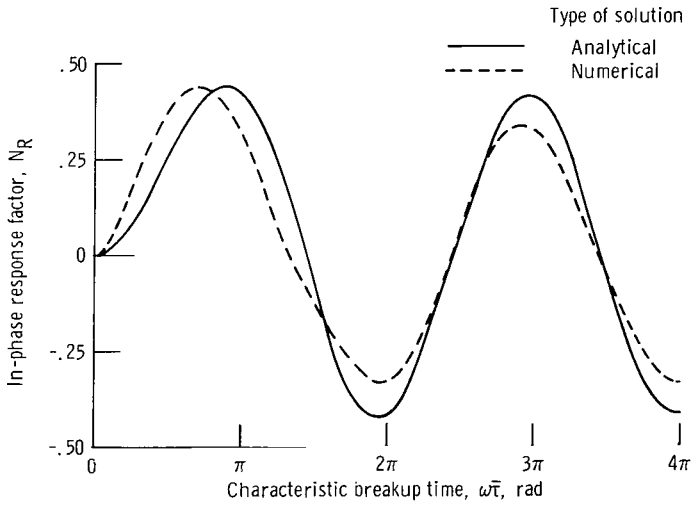

Figure 17. - Response at angular position of $\pi/4$ radians and radial position of 1.0 in standing mode. Steady velocity difference, 0; pressure amplitude, 0.1; speed of sound, 5000 feet per second (1520 m/sec); ratio of specific heats, 1.2.

a stabilizing effect and a u_R velocity a destabilizing effect on a combustion system sensitive to jet atomization.

The depressive effect of an out-of-phase velocity on response is more clearly shown in figure 18. Analytical values of $(N_R)_{max}$ are shown as a function of $\hat{P}'$ and $|u_l - u_z|$ for the quarter wave wall position. The characteristics shown in figure 18 are an inversion of a similar variation for the traveling wave shown in figure 11. For a given value of $|u_l - u_z|$ in this standing mode N_R has an asymptotic maximum at low pressure amplitudes and an asymptotic minimum at high amplitudes. The suppressive effect of an out-of-phase velocity is most severe at high pressure amplitudes and low values of $|u_l - u_z|$. Numerical solutions gave similar trends but the suppressive effect is more severe as shown in figure 18.

Similar properties of $(N_R)_{max}$ are exhibited at all other positions within the standing mode except for the constant value of $(N_R)_{max}$ of $1/\gamma$ occurring at the velocity node. The pressure node is no exception even though pressure oscillation disappears. In a system analysis for stability, however, the response at a pressure node usually becomes insignificant because system integrals essentially weight the response by the pressure amplitude.

Generalizing the response in the standing mode is difficult. Response varies with both angular and radial position and causes complex patterns of response factors distri-

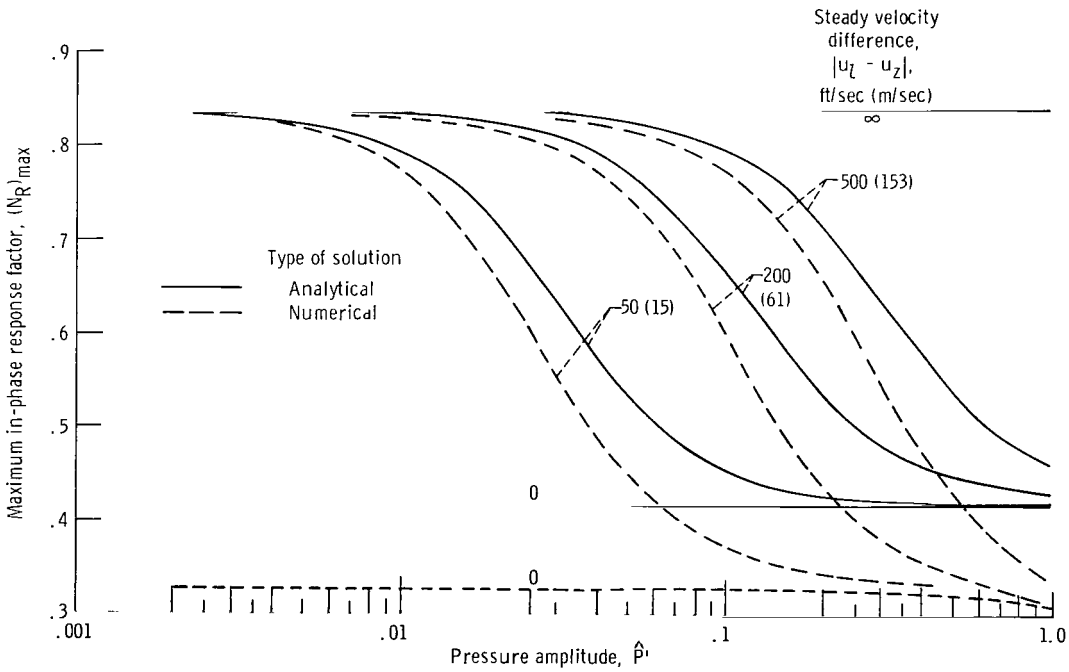

Figure 18. - Maximum in-phase response factor at angular position of $\pi/4$ radians and radial position of 1.0 in standing mode. Speed of sound, 5000 feet per second (1520 m/sec); ratio of specific heats, 1.2. Maximum values near $\omega\bar{\tau} = 3\pi$ used for comparison.

buted across the cross section. The maximum average value of either N_R or N_I in the standing mode, however, will always be less than for the traveling mode.

Radial Acoustic Mode

The first order terms for the properties of the radial mode are given by

$$P = \bar{P}\left[1 + A\gamma J_0(\beta)\cos\ \omega t\right] \tag{44}$$

$$\rho_g = \bar{\rho}_g\left[1 + AJ_0(\beta)\cos\ \omega t\right] \tag{45}$$

$$u_r = -Ac\beta J_1(\beta)\sin\ \omega t \tag{46}$$

where

$$\beta = 3.83\ r$$

Radial velocities are out-of-phase with pressure and there are no angular velocities. The identities become

$$\left.\begin{aligned} u_I &= u_r \\ \hat{u}_I &= -\frac{c\hat{P}'}{\gamma}\left[\beta\frac{J_1(\beta)}{J_0(\beta)}\right] \\ \hat{P}' &= A\gamma J_0(\beta) \end{aligned}\right\} \tag{47}$$

Maximum values of N_R and N_I for the radial mode are contained within the same limits as for the standing mode. At the wall and center, where velocity perturbations vanish, $(N_R)_{max}$ is $1/\gamma$. At other positions $(N_R)_{max}$ can be reduced to about $\frac{1}{2}\gamma$ analytically and 0.33 numerically because of the suppressive effect of an out-of-phase velocity component.

As in the case of the other modes, velocity perturbations can cause breakup time to vary with radial position and substantially effect the values of N_R and N_I. Figure 19 compares changes in $\bar{\tau}$ with radial position for the different modes. The comparison is for $|u_l - u_z|$ equal to 100 feet per second (30.5 m/sec) and a maximum pressure ampli-

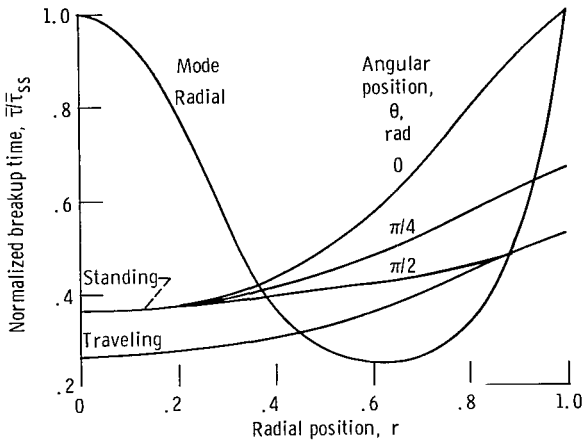

Figure 19. - Comparison of normalized breakup time variations for various acoustic modes. Maximum pressure amplitude, 0.1 at radial position of 1.0 for all modes. Steady velocity difference, 100 feet per second (30 m/sec).

tude at the wall of 0.1 for all modes. For the radial mode $\omega\bar{\tau}$ attains a minimum value at the pressure node. The traveling mode exhibits the smallest total change in $\omega\bar{\tau}$ when considering both radial and angular position. Considering this distinction in addition to the lower peak values of N_R in the standing and radial modes further implicates the traveling mode as potentially most unstable. Large changes in $\omega\bar{\tau}$ and the accompanying changes in N_R can severely degrade the potential of the standing and radial modes for high response. This does not imply that space averaged response factors are always the largest in traveling modes.

EFFECT OF DISTRIBUTED PROPERTIES

The preceding analyses have shown the dynamic properties of a discrete breakup process in which all elements of a jet breakup when distortion attains a constant critical value. Breakup of an actual jet, however, rather than being discrete is distributed in both time and space as shown in figure 6. Such distributed properties will affect the dynamic response. For example, figure 6 shows the time interval during which breakup occurs to be proportional to the mean breakup time. If the mean breakup time is large, the large time interval of breakup and mass release could encompass several cycles of acoustic oscillation. Response for such a condition would be small because the time correlation between mass release rate and pressure oscillations (a basic property of response factors) is small. Similarly, increasing the frequency would eventually decrease the correlation and reduce the response. This implies that the response factors N_R and N_I should decrease with increasing values of $\omega\bar{\tau}$. The response of discrete breakup

(eq. (29) and (30) and fig. 7) does not exhibit such properties. Rather, the response factors beyond an $\omega\bar{\tau}$ of about 4π radians become simple periodic functions of constant amplitude. Dynamic properties of a discrete breakup process, therefore, do not characterize those of the actual process when $\omega\bar{\tau}$ is large.

In the following analysis the modifying effects of a distributed process on the dynamic properties of a discrete process are examined in an attempt to more realistically model the actual characteristics of jet breakup.

For the purpose of analysis, a multiplicity of identical jets are assumed in a common environment. The dynamic properties of each jet are those of a discrete breakup process. The critical value of distortion ϵ identified with breakup, however, is a distinguishing feature of each jet. The population density of jets as a function of the breakup time τ is chosen to be the mass release distribution with τ shown in figure 6.

The mass release rate in-phase with the pressure oscillation N_R for any jet is given by equation (29). Since pressure disturbances are identical for each jet in the common environment, the average value of the mass release rate in-phase with pressure for the multiplicity of jets is the integral average of the individual values of N_R. Approximating the population density of jets by a uniform distribution with outer boundaries of $\pm\sigma$, the equation for the average response is given by

$$\frac{\gamma}{\hat{V}'} N_R = \frac{1}{2\sigma\omega\bar{\tau}} \int_{\omega\bar{\tau}(1-\sigma)}^{\omega\bar{\tau}(1+\sigma)} \left(\frac{\sin \omega\bar{\tau}}{\omega\bar{\tau}} - \cos \omega\bar{\tau}\right) d\omega\bar{\tau} \tag{48}$$

The solution to equation (48), where the integration of the first term is given by a series expression, is

$$\frac{\gamma}{\hat{V}'} N_R = \left[1 - \frac{(\omega\bar{\tau})^2}{3!}\left(1 + \frac{\sigma^2}{3}\right) + \frac{(\omega\bar{\tau})^4}{5!}\left(1 + 2\sigma^2 + \frac{\sigma^4}{5}\right) - \frac{(\omega\bar{\tau})^6}{7!}\left(1 + 5\sigma^2 + 3\sigma^4 + \frac{\sigma^6}{7}\right)\cdots\right] - \frac{\sin \sigma\omega\bar{\tau}}{\sigma\omega\bar{\tau}} \cos \omega\bar{\tau} \tag{49}$$

When σ is small, the solution can be approximated by

$$\frac{\gamma}{\hat{V}'} N_R = \frac{\sin \sigma\omega\bar{\tau}}{\sigma\omega\bar{\tau}} \left(\frac{\sin \omega\bar{\tau}}{\omega\bar{\tau}} - \cos \omega\bar{\tau}\right) \tag{50}$$

Similarly, the average value of N_I is approximated by

$$\frac{\gamma}{V'} N_I = \frac{\sin \sigma\omega\bar{\tau}}{\sigma\omega\bar{\tau}} \left(\frac{1 - \cos \omega\bar{\tau}}{\omega\bar{\tau}} - \sin \omega\bar{\tau} \right) \tag{51}$$

The term $\sin \sigma\omega\bar{\tau}/\sigma\omega\bar{\tau}$ is a converging period function which modifies the response expressions for the discrete breakup process. A value of σ of 0.15 encompasses 50 percent of the mass release for the distribution curve of figure 5. Using a σ of 0.15 to characterize the distribution, the modified response function given by equations (50) and (51) are shown in figure 20. With the modified response functions, the peak values

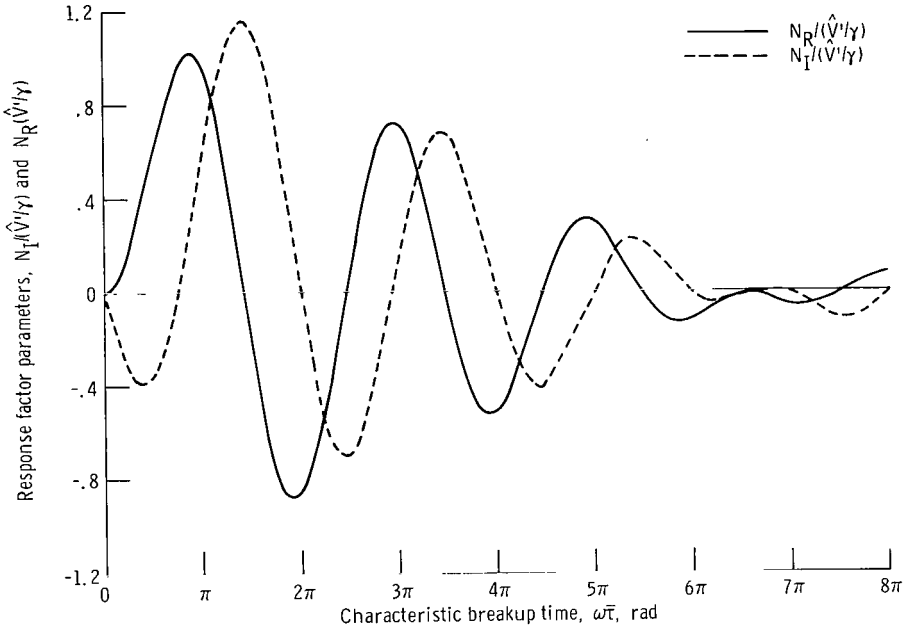

Figure 20. - Response for distributed jet breakup process. Deviation parameter, $\omega\sigma$, 0.15.

decrease with an increase in $\omega\bar{\tau}$, the type of behavior expected from an actual jet atomization process.

Accepting the modified response functions as more characteristic of the actual process does not particularly alter the previous discussion of the discrete process in specific acoustic modes. The initial maximum value of these periodic response functions is not significantly affected in the modified functions and is comparable to the value at $\omega\tau = 3\pi$ used previously in figures 11 and 18 as an index of the potential response.

The properties of a distributed process emphasize the difficulties to be expected in experimental observations of jet dynamics. The breakup is obscure because it is distributed in both length and time. Distributed breakup also reduces the magnitude of any change in atomization rate. In addition, the dynamic properties of primary importance

are related to the first harmonic content of these distributed properties. Indeed, the prospect for reliable dynamic data from direct measurements of jet length properties seem remote.

EFFECT OF VORTEX FLOW

Vortex flow was a primary variable in the two-dimensional combustor studies of liquid jet behavior during instability shown in figures 2 to 4. In these studies, the degree of instability was related to the degree of vortex flow. This implies that dynamic response of the combustion process is affected by a steady angular flow. Analytical studies (refs. 15 to 17) have shown that a steady velocity can enhance the dynamic response of a velocity sensitive process. An analysis of the effect of a steady angular velocity on the jet breakup process will show that a significant increase in dynamic response can also be expected.

Limiting the analysis to a wall position in a traveling transverse-acoustic mode (simulating the two-dimensional combustor studies), the forcing function f(t) for equation (13) takes the form

$$f(t) = \rho_g\left(|u_l - u_z|^2 + u_\theta^2\right) \tag{52}$$

where

$$P(t) = \bar{P}(1 + \hat{P}' \cos \omega t)$$

$$\bar{\rho}_g(t) = \bar{\rho}_g\left(1 + \frac{1}{\gamma}\hat{P}' \cos \omega t\right)$$

$$u_\theta(t) = \bar{u}_\theta + \frac{c}{\alpha}\frac{\hat{P}'}{\gamma}\cos \omega t$$

Using these properties and extracting the first harmonic content of f(t) gives

$$f(t) = \bar{\rho}_g\left(V_{rms}\right)_{\bar{\theta}}^2\left(1 + V'_{\bar{\theta}}\frac{P'}{\gamma}\cos \omega t\right) \tag{53}$$

where

$$\hat{V}'_{\bar{\theta}} = \frac{|u_l - u_z|^2 + \bar{u}_\theta^2 + \frac{3}{4}\left(\frac{c\hat{P}'}{\alpha\gamma}\right)^2 + 2\frac{c\bar{u}_\theta}{\alpha}}{|u_l - u_z|^2 + \bar{u}_\theta^2 + \frac{1}{2}\left(\frac{c\hat{P}'}{\alpha\gamma}\right)^2 + \left(\frac{\hat{P}'}{\gamma}\right)^2 \frac{cu_\theta}{\alpha}} \tag{54}$$

$$\left(V_{rms}\right)_{\bar{\theta}} = |u_l - u_z|^2 + \bar{u}_\theta^2 + \frac{1}{2}\left(\frac{c\hat{P}'}{\alpha\gamma}\right)^2 + \left(\frac{\hat{P}'}{\gamma}\right)^2 \frac{c\bar{u}_\theta}{\alpha} \tag{55}$$

The two response factors are of the same functional form as in equations (29) and (30) Including the modifying effect of a distributed process, they are

$$N_R = \frac{\hat{V}'_{\bar{\theta}}}{\gamma} \frac{\sin \sigma\omega\bar{\tau}}{\sigma\omega\bar{\tau}} \left(\frac{\sin \omega\bar{\tau}}{\omega\bar{\tau}} - \cos \omega\bar{\tau}\right) \tag{56}$$

$$N_I = \frac{\hat{V}'_{\bar{\theta}}}{\gamma} \frac{\sin \sigma\omega\bar{\tau}}{\omega\bar{\tau}} \left(\frac{1 - \cos \omega\bar{\tau}}{\sigma\omega\bar{\tau}} - \sin \omega\bar{\tau}\right) \tag{57}$$

The mean breakup time $\omega\bar{\tau}$ is given by

$$\omega\bar{\tau} = \frac{D\omega}{\left(V_{rms}\right)_{\bar{\theta}}} \left(\frac{\rho_l}{\rho_g} \epsilon\right)^{1/2} \tag{58}$$

The converging periodic nature of both N_R and N_I with $\omega\bar{\tau}$ is identical to that previously discussed and shown in figure 20. The steady angular velocity u_θ, however, affects the modifying factor $\hat{V}'_{\bar{\theta}}/\gamma$ and thereby significantly affects the magnitude of the response. Mean breakup time is also sensitive to the angular velocity. These affects are best illustrated by a specific example.

The conditions citied in reference 8 for the oxygen jet breakup process shown in figure 3 are

Jet diameter, D, in.; m	0.028; 0.00071
Average angular velocity, $\bar{u}_\theta$, ft/sec; m/sec	235; 72
Liquid density, ρ_l, lbm/ft^3; kg/m^3	75; 1200
Gas density, ρ_g, lbm/ft^3; kg/m^3	0.1; 1.6
Liquid velocity, μ_l, in./sec, m/sec	360; 9.2
Average radial velocity, in./sec; m/sec	1140; 29
Frequency, ω, rad/sec	27 300
Speed of sound, c, ft/sec; m/sec	4720; 144
Pressure ratio, $\Delta P_{p\text{-}p}/\overline{P}$	0.667

For $\bar{u}_r \equiv \bar{u}_z$ in equations (54) and (55), a characteristic time $\omega\bar{\tau}$ of 2860 radians and a jet length of 0.72 inch (0.018 m) are predicted for the case of no angular velocity, and $\epsilon = 3.5$. Figure 21 shows the effect of a steady tangential velocity on breakup time and jet length for several pressure amplitudes. As the tangential velocity increases to 300 feet per second (72 m/sec), the breakup time is reduced to the period of about $1\frac{1}{2}$ cycles of acoustic oscillation where a significant response from the breakup process is anticipated. The peak magnitude of the response factors is approximated by $\hat{V}'_\theta/\gamma$,

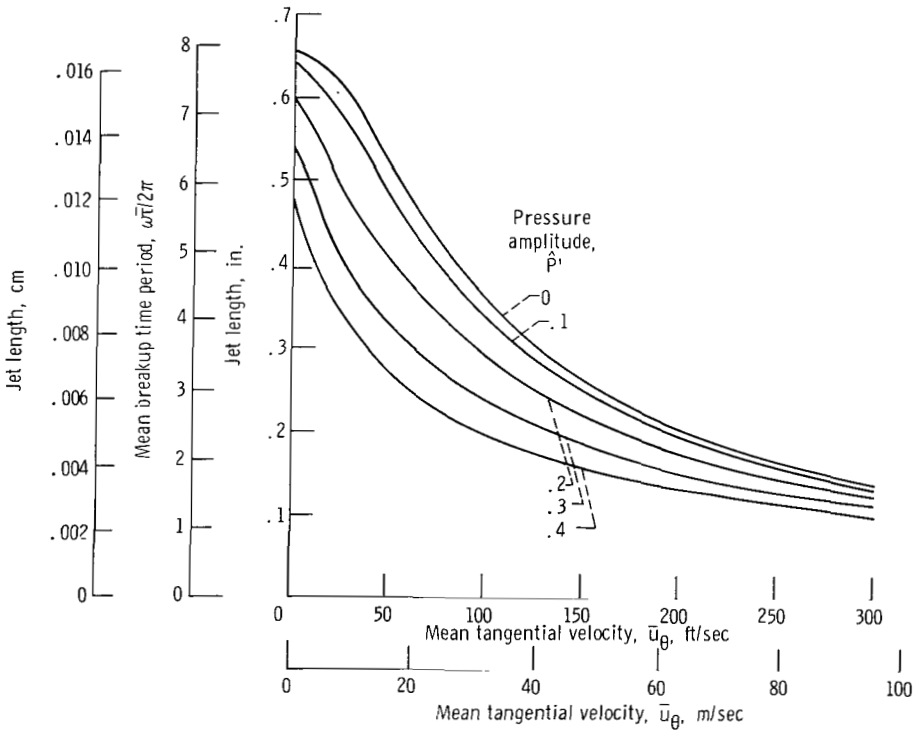

Figure 21. - Calculated effect of tangential velocity and pressure amplitude on jet length and mean breakup time for test conditions of reference 8.

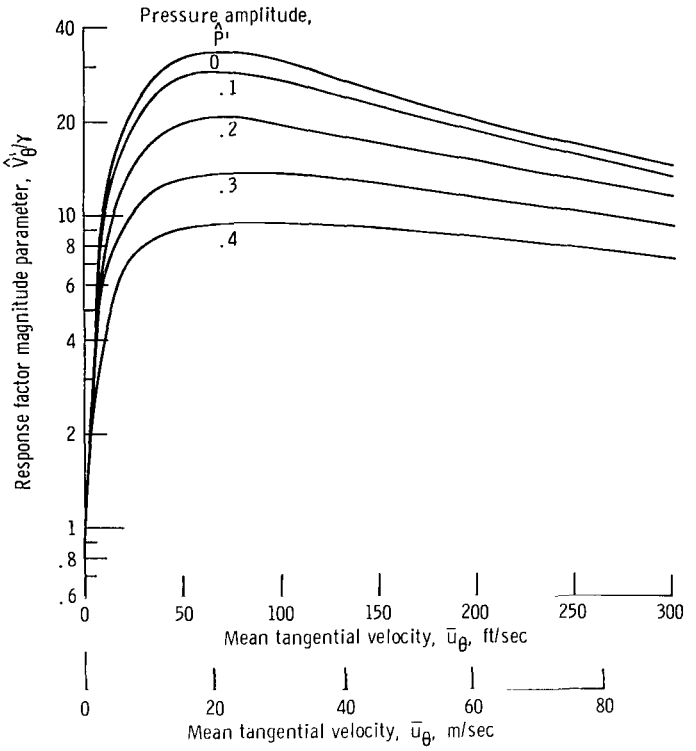

Figure 22. - Calculated effect of tangential velocity and pressure amplitude on response magnitude for test conditions of reference 8.

which is also dependent on $u_{\overline{\theta}}$. This is shown in figure 22. The amplifying effect of $u_{\overline{\theta}}$ on response is substantial. The response factors can be increased by more than an order of magnitude over that for no steady tangential velocity when the response factor is near unity.

The specific pressure amplitude for the jet conditions of this example are not directly applicable to the dynamic analysis because the pressure waveform is strongly nonlinear. A sinusoidal wave amplitude of $\hat{P}' = 0.3$, which is the approximate first harmonic content of the actual wave, may be representative. For $\hat{P}' = 0.3$ and $\bar{u}_\theta = 235$ feet per second (72 m/sec), an $\omega\tau/2\pi$ of 1.65 and $\hat{V}'_\theta/\gamma$ of 10.8 are given by figures 21 and 22. These values prescribe response factors of 4.0 for N_R and 6.5 for N_I which would usually imply a highly unstable condition.

The effects of $\bar{u}_\theta$ on N_R are more clearly shown in figure 23. For a constant amplitude of 0.3, an increase in $\bar{u}_\theta$ is shown to cause periodic variations in N_R of increasing amplitude. The major region of positive response occurs for tangential velocities above 220 feet per second (67 m/sec) and encompasses the reference 8 test condition.

The effect of pressure amplitude on response for a tangential velocity of 235 feet

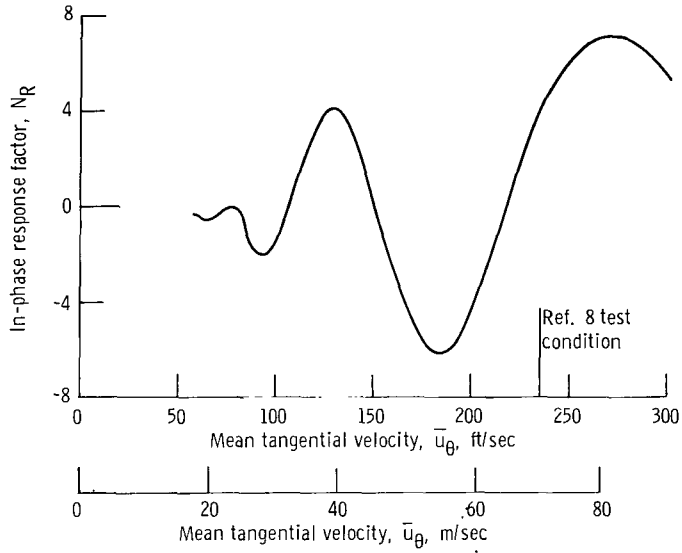

Figure 23. - Calculated effect of tangential velocity on in-phase response factor for pressure amplitude of 0.3 and other jet conditions of reference 8.

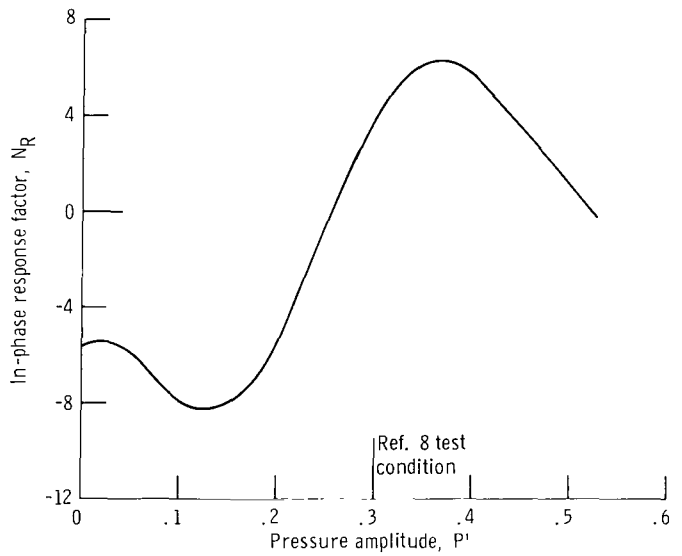

Figure 24. - Calculated effect of pressure amplitude on in-phase response factor for mean tangential velocity of 235 feet per second (71 m/sec) and other jet conditions of reference 8.

per second (72 m/sec) is shown in figure 24. Positive response and potential instability is indicated for the reference 8 pressure amplitude of 0.3. Figures 23 and 24, imply unstable combustion in regions other than the test condition of reference 8. Experimentally (refs. 7 and 14), pressure amplitude increased uniformly with $\bar{u}_\theta$. A stability analysis of the complete system is required, however, to establish the relation between equilibrium amplitude and combustion response.

SUMMARY OF RESULTS

The dynamic response of a liquid jet atomization process within traveling, standing, and radial transverse acoustic modes was derived by both theoretical and numerical analyses. The response was characterized by two response factors: the in-phase N_R and out-of-phase N_I components of atomization rate perturbations with respect to pressure perturbations. A characteristic breakup time $\omega\bar{\tau}$ (the product of jet breakup time and frequency) was an important correlating parameter for the response factors. Results of the analysis are as follows:

1. For all cases, the response factors N_R and N_I were periodic functions of the characteristic breakup time $\omega\bar{\tau}$. The amplitude of the periodicity converges with an increase in $\omega\bar{\tau}$ when a breakup process distributed along the jet length is considered. The maximum values of N_R and N_I occur at values of $\omega\bar{\tau}$ of about π and $3\pi/2$ radians, respectively, with secondary peaks occurring at intervals of about 2π radians. Convergence of the periodic function implies that large increases in jet diameter or oscillatory frequency would stabilize a combustion system.

2. The magnitude of the peak values of the response factors varied with acoustic conditions. Values of N_R as large as 1.25 for the traveling mode and 0.833 for the standing and radial mode were obtained by theoretical analysis. The numerical analysis, which preserved all nonlinear effects, gave a larger value of 1.51 for the traveling mode. Comparable values were obtained for N_I.

3. Variations in the peak values of the response factors are caused by the velocity sensitivity of the atomization process. Pressure sensitivity alone gave a peak value of 0.833. A velocity perturbation in-phase with the pressure elevated the peak value and is destabilizing to a combustion system. An out-of-phase velocity perturbation reduced the peak value and is stabilizing. A large steady relative velocity difference between the liquid and gas suppresses these velocity effects and causes the response to approach the pressure sensitive value.

4. Spacial variations of acoustic properties within a given mode can cause large variations in local dynamic properties. The most severe effects on response factors are caused by the effect of acoustic properties on mean jet breakup time, which varies in-

versely with the magnitude of the local velocity perturbations. Response factors are periodic functions of breakup time and thus vary spatially throughout the mode. Such varied response precludes any simple characterization of the average response in a given mode. Potentially, however, the maximum average response for the traveling mode is larger than for either the standing or radial modes. Average response also depends on the uniformity of the injection pattern and may account for the effect of nonuniform injection on stability observed experimentally.

5. The amplifying effect of a steady vortex velocity on the response of the jet atomization process is substantial. Peak response factors can be increased by an order of magnitude. The result may explain the instability encountered in a circular research combustor with vortex flow. Quantitative evaluations for one test condition showed jet response characteristics consistent with the experimental observations.

Lewis Research Center,
National Aeronautics and Space Administration,
Cleveland, Ohio, April 9, 1969,
128-31-51-02-22.

APPENDIX - SYMBOLS

A	amplitude coefficients, eqs. (37), (43), and (47), dimensionless
a	acceleration, ft/sec^2; m/sec^2
c	speed of sound, ft/sec; m/sec
D	jet diameter, ft; m
J_n	Bessel function of the first kind of order n
N	response factor, component of w'/P', dimensionless
P	pressure, psi; N/m^2
r	fraction of combustor radius or radial position, dimensionless
t	time, sec
u	velocity, ft/sec; m/sec
V	magnitude of relative velocity vector, ft/sec; m/sec
w	mass flow rate, lbm/sec; kg/sec
α	radius parameter, 1.841 r
β	radius parameter, 3.83 r
γ	ratio of specific heats, dimensionless
δ	jet distortion, ft; m
ϵ	relative distortion, δ/D
θ	angular position, radians
ρ	density, lb/ft^3; kg/m
σ	deviation from mean, dimensionless
τ	jet breakup time, sec
ω	frequency, rad/sec

Subscripts:

g	gas
I	imaginary or out-of-phase component
l	liquid
p-p	peak-to-peak
R	real or in-phase component
r	radial component
rms	root mean square
ss	steady-state
z	axial component
θ	angular component
0	initial

Superscripts

$\bar{}$	mean or average value
$\hat{}$	maximum value
'	perturbation about mean

REFERENCES

1. Heidmann, Marcus F.; and Wieber, Paul R.: Analysis of Frequency Response Characteristics of Propellant Vaporization. NASA TN D-3749, 1966.
2. Crocco, L.; et al.: Nonlinear Aspects of Combustion Instability in Liquid Propellant Rocket Motors. Rep. AMS-SR-553-g, Princeton Univ. (NASA CR-72270), June 1967.
3. Feiler, Charles E.; and Heidmann, Marcus F.: Dynamic Response of Gaseous-Hydrogen Flow System and Its Application to High-Frequency Combustion Instability. NASA TN D-4040, 1967.
4. Wanhainen, John P.; Feiler, Charles E.; and Morgan, C. Joe: Effect of Chamber Pressure, Flow per Element, and Contraction Ratio on Acoustic-Mode Instability in Hydrogen-Oxygen Rockets. NASA TN D-4733, 1968.
5. Strahle, Warren C.: A Theoretical Study of Unsteady Droplet Burning: Transients and Periodic Solutions. Aeron. Eng. Rep. 671, Princeton University. (NASA CR-55516), 1963.
6. Dykema, O. W.: An Engineering Approach to Combustion Instability. Rep. TDR-669 (6126-22)-1, Aerospace Corp. (SSD-TR-65-177, DDC No. AD-475934), Nov. 5, 1965.
7. Heidmann, Marcus F.: Oxygen-Jet Behavior During Combustion Instability in a Two-Dimensional Combustor. NASA TN D-2725, 1965.
8. Heidmann, Marcus F.: Oscillatory Combustion of a Liquid-Oxygen Jet With Gaseous Hydrogen. NASA TN D-2753, 1965.
9. Clark, Bruce J.: Breakup of a Liquid Jet in a Transverse Flow of Gas. NASA TN D-2424, 1964.
10. Burrows, Marshall C.: Dynamic Response of Hydrazing-Nitrogen Tetroxide Combustion to Transverse Gas Flow. NASA TN D-4984.
11. Dabora, E. K.; Ragland, K. W.; Ranger, A. A.; and Nicholls, J. A.: Detonations in Two-Phase Media and Drop Shattering Studies. Rep. UM-06324-5-T, University of Michigan. (NASA CR-72421), May 1968.
12. Buffum, F. G.; and Williams, F. A.: The Response of a Turbulent Liquid Jet to Transverse Acoustic Fields. Proceedings of the 1967 Heat Transfer and Fluid Mechanics Institute. P. A. Libby, D. B. Olfe, and C. W. Van Atta, eds., Standford University Press, 1967, pp. 247-276.

13. Priem, Richard J.; and Rice, Edward J.: Combustion Instability with Finite Mach Number Flow and Acoustic Liners. Presented at the Twelfth Symposium (international) on Combustion, Poitiers, France, July 1968.

14. Heidmann, Marcus F.; and Groeneweg, John F.: Dynamic Response of Liquid Jet Breakup. AIAA J. vol. 6, no. 10, Oct. 1968, pp. 2033-2035.

15. Heidmann, Marcus F.; and Feiler, Charles E.: Evaluation of Tangential Velocity Effects on Spinning Transverse Combustion Instability. NASA TN D-3406, 1966.

16. Priem, Richard J.; and Rice, Edward J.: Combustion Instability with Finite Mach Number Flow and Acoustic Liners. Presented at the Twelfth Symposium (International) on Combustion, Poitiers, France, July 1968.

17. Povinelli, Louis A.; Heidmann, Marcus F.; and Feiler, Charles E.: Experimental Investigation of Transverse - Mode Solid-Propellant Combustion Instability in a Vortex Burner. NASA TN D-3708, 1966.

NASA-Langley, 1969 —— 28 E-4998

"The aeronautical and space activities of the United States shall be conducted so as to contribute . . . to the expansion of human knowledge of phenomena in the atmosphere and space. The Administration shall provide for the widest practicable and appropriate dissemination of information concerning its activities and the results thereof."

—NATIONAL AERONAUTICS AND SPACE ACT OF 1958

NASA SCIENTIFIC AND TECHNICAL PUBLICATIONS

TECHNICAL REPORTS: Scientific and technical information considered important, complete, and a lasting contribution to existing knowledge.

TECHNICAL NOTES: Information less broad in scope but nevertheless of importance as a contribution to existing knowledge.

TECHNICAL MEMORANDUMS: Information receiving limited distribution because of preliminary data, security classification, or other reasons.

CONTRACTOR REPORTS: Scientific and technical information generated under a NASA contract or grant and considered an important contribution to existing knowledge.

TECHNICAL TRANSLATIONS: Information published in a foreign language considered to merit NASA distribution in English.

SPECIAL PUBLICATIONS: Information derived from or of value to NASA activities. Publications include conference proceedings, monographs, data compilations, handbooks, sourcebooks, and special bibliographies.

TECHNOLOGY UTILIZATION PUBLICATIONS: Information on technology used by NASA that may be of particular interest in commercial and other non-aerospace applications. Publications include Tech Briefs, Technology Utilization Reports and Notes, and Technology Surveys.

Details on the availability of these publications may be obtained from:

SCIENTIFIC AND TECHNICAL INFORMATION DIVISION

NATIONAL AERONAUTICS AND SPACE ADMINISTRATION

Washington, D.C. 20546